ÇUKUROVA UNIVERSITY
INSTITUTE OF NATURAL AND APPLIED SCIENCES

MSc THESIS

Fulya KARAÇORA NANE

INVESTIGATION OF ASYMMETRIC TRANSMISSION PROPERTIES IN 2-D PHOTONIC CRYSTALS

DEPARTMENT OF ELECTRICAL AND ELECTRONICS ENGINEERING

ADANA-2018

ÇUKUROVA UNIVERSITY
INSTITUTE OF NATURAL AND APPLIED SCIENCES

INVESTIGATION OF ASYMMETRIC TRANSMISSION PROPERTIES IN 2-D PHOTONIC CRYSTALS

Fulya KARAÇORA NANE

MSc THESIS

DEPARTMENT OF ELECTRICAL AND ELECTRONICS ENGINEERING

We certified that the thesis titled above was reviewed and approved for the award of degree of Master of Philosophy by the board of jury on 02/08/2018.

Prof. Dr. Turgut İKİZ	Prof. Dr. Bekir ÖZÇELİK	Ast. Prof. Dr. Şule ÇOLAK
SUPERVISOR	MEMBER	MEMBER

This MSc. Thesis is performed in Department of Institute of Basic and Applied Sciences of Çukurova University.
Registration Number:

Prof. Dr. Mustafa GÖK
Director
Institute of Natural and Applied Sciences

ABSTRACT

MSc. THESIS

INVESTIGATION OF ASYMMETRIC TRANSMISSION PROPERTIES IN 2-D PHOTONIC CRYSTALS

Fulya KARAÇORA NANE

ÇUKUROVA UNIVERSITY
INSTITUTE OF NATURAL AND APPLIED SCIENCES DEPARTMENT OF ELECTRICAL - ELECTRONICSENGINEERING

Supervisor : Prof. Dr. Turgut İKİZ
Year: 2018, Pages: 53
Jury : Prof. Dr. Turgut İKİZ
: Prof. Dr. Bekir ÖZÇELİK
: Asst. Prof. Dr. Şule ÇOLAK

This study is theoretical investigation on the properties of asymmetric transmission in 2-D photonic crystals. In particular, this thesis concerns the transmittance of terahertz waves on metallic dual layers. The effects of different geometric and optical parameters on the transmission are investigated by using MATLAB and freely available MEEP software based on the FDTD method.

The three different structures made of silver are used to manipulate electromagnetic propagation of different wave lengths. The simulation results represent transmittance values for the TM mode where the electromagnetic propagation transverse to the same way of incidence wave. As a result, the best comparative asymmetric transmittance values are obtained as 0.75, and 0.15 from top and bottom sides, respectively.

Key Words: 2-D Photonic Crystal, Asymmetric Transmission, FDTD.

ÖZ

YÜKSEK LİSANS TEZİ

İKİ BOYUTLU FOTONİK KRİSTALLERDE ASİMETRİK GEÇİŞ ÖZELLİKLERİNİN ARAŞTIRILMASI

Fulya KARAÇORA NANE

ÇUKUROVA ÜNİVERSİTESİ
FEN BİLİMLERİ ENSTİTÜSÜ
ELEKTRİK ELEKTRONİK MÜHENDİSLİĞİ BÖLÜMÜ

Danışman : Prof. Dr. Turgut İKİZ
Yıl: 2018, Sayfa: 53
Jüri : Prof. Dr. Turgut İKİZ
: Prof. Dr. Bekir ÖZÇELİK
: Dr. Öğr. Üyesi. Şule ÇOLAK

Bu çalışma 2-boyutlu fotonik kristallerde asimetrik geçiş özellikleri üzerine teorik bir araştırmadır. Bu tezde özellikle terahertz dalgalarının iki katmanlı metalik yapılarda iletimi üzerinde durulmuştur. Çalışmada farklı geometrik ve optik parametrelerin geçirgenlik üzerindeki etkileri FDTD tabanlı MATLAB ve ücretsiz MEEP programı aracılığı ile araştırılmıştır.

Farklı dalga boylarında elektromanyetik yayınımı kontrol etmek için 3 farklı geometriye sahip gümüş tasarım kullanılmıştır. Simülasyon sonuçları gelen dalga ile aynı yönde iletilen elektromanyetik yayınım için TM modunda geçirgenlik katsayı değerlerini vermektedir. Çalışma sonucunda en iyi asimetrik geçirgenlik katsayı değerleri 0.75 (üstten gelen) ve 0.15 (alttan gelen) olarak elde edilmiştir.

Anahtar Kelimeler: 2-Boyutlu Fotonik Kristal, Asimetrik Geçirgenlik, Zamanda Sonlu Farklar Metodu.

EXPANDED ABSTRACT

All electronic gadgets like transistors use electrical signals made of electrons moving from one place to another one for communication. Use of light instead of electricity has been considered to be one of the most promising solutions to make electronic components even faster. The main advantage of light is the fastest thing you can use to process and transfer information. Already, fiber optic cables, which simply guide light, are used in current telecommunication technologies.

In recent years, there is widespread research interest in optoelectronics made of optical systems and devices. This area is also called as Photonics, which is a collaborative area of electrical and electronics engineering, material science, physics, and optics. At present, optical integrated circuits using light propagation are being studied and developing intensively. To develop the light based electronic components and devices, it is necessary to create the useful optical materials by giving us a chance to controlling of wave propagation.

This study focuses on the investigation of asymmetric transmission properties of novel dual metallic photonic crystals. The method used in this study is FDTD method. The effects of different geometric and optical parameters on the transmission are investigated by using MATLAB and freely available MEEP software(MIT Electromagnetic Equation Propagation) based on the FDTD method.The three different structures made of silver are used to manipulating electromagnetic propagation of different wave lengths. The simulation results represent transmittance values for the TM mode where the electromagnetic propagation transverse to the same way of incidence wave.

In this thesis, we investigated asymmetric transmission properties of two dimensional metallic gratings for optoelectronic applications. We tried to obtain asymmetric propagation behavior by changing the geometry of metallic grating. According to reference paper (M. Stolarek, 2013: Cheng, 2007: Cheng, 2008: Xu,

2011), we have considered some dual metal geometries and studied the transmission spectrum of these structures by freely available MEEP program. We have also compared the MEEP's simulation results by MATLAB. MEEP implements the FDTD method for computational electromagnetism. FDTD algorithm is today's most popular calculation tools (Taflove, 2000). The time and space are divided in a uniform grid for FDTD algorithm which solves time dependent Maxwell equations. For determination of boundary conditions, Perfect matched layer PML is embedded in the simulation (Berenger, 1994). Generally, the width of PML layer is equal to a lattice constant in overall simulation area. FDTD solves time-space dependent magnetic and electric fields in different spatial regions by sliding electric and magnetic field components. This idea of grid discretization was first proposed by Yee (Yee, 1966). Fields in grids can be classified as TM and TE polarization.

The outline of this thesis is as fallows. In the first chapter, an introduction to some basics of photonic crystals, optoelectronics, and applications of photonic crystal in optoelectronics is given. Chapter 2 describes the fundamental concepts of our work. The method of analysis we used and problem definition are explained in chapter 3. Numerical results of TM mode analysis obtained by MEEP software and MATLAB are presented in chapter 4. Chapter 5 contains conclusion and scope of future work.

The scheme of our simulation setup for the investigation on the asymmetric transmission of light in our dual metal grating designs is given in numerical method section. The unidirectional transmittances of terahertz wave's incidence from top side and bottom side were obtained in TM mode. The transmission spectrums of all designs are calculated for different values of G parameter (distance between dual metallic layers) in TM mode and plotted versus wavelength. In this simulation, we use perfectly matched layer PML (Berenger, 1994) boundary conditions which absorbs electromagnetic waves at the boundaries without reflections. Here, interference waves are sinusoidal wave. The dual metal structures were embedded in free space (ϵ=μ=1) surrounded by PML. The MEEP simulation results were also checked with snapshots of wave propagation obtained by MATLAB for same design structures. Procedure of FDTD and calculating transmittance was provided as below. The sizes of metal gratings chosen for three different designs are given in result section and these three different designs are hereafter named as design A, design B, and design C, respectively.

Procedure of Calculating Transmission and Reflection Coefficients;

1. Performing FDTD based simulation
   a. Calculating the steady state field in the region where reflection and transmission are observed
2. For selected frequency
   a. Calculating the wave vector components of the spatial harmonics
   b. Calculating the complex amplitude of the spatial harmonics
   c. Calculating the diffraction efficiency of the spatial harmonics
   d. Calculating over all reflection and transmission coefficient
   e. Calculating conservation of energy

As a result, the aim of this thesis was to obtain an asymmetric transmission behavior in the 2-D dual metallic photonic crystals. For this purpose, we designed three novel dual metallic structures and analyzed the numerical results of electromagnetic wave propagation for TM mode. Firstly, the distance between dual metallic layers was modified to obtain the asymmetric transmission. It is possible to say that we could not obtain an effective asymmetric transmission behavior for our design A and B. Nevertheless, we have carried out an asymmetric transmission behavior in design C for a large range of wavelength for all G values. We have also checked the most effective parameters of design C (G=200nm, λ= 2.9 μm) by MATLAB simulations. The MATLAB results are consistent with the MEEP results. As a further work, we have studied on the effects of an intermediate dielectric material between dual metallic layer of design C for G=200 nm. But the transmission spectrum results show that the intermediate material has demolished the behavior of asymmetric transmission in the structure of design C.

The asymmetric transmission means that an electromagnetic propagation is completely transmitted in one direction, but blocked in other direction. This feature can be utilized to design the optical diodes (Scalora, 1994) for light based integrated circuits. Consequently, the transmission spectrum of design C reveals optical diode like transmission behavior around 3 µm. There are many studies on such optical diodes (Biancalana, 2008: Wang, 2011: Kurt, 2012: Stolarek, 2013). Although our goal is to achieve an asymmetric transmission behavior, the design A and B show a sharp filtering feature (Wang, 1995: Hu, 2015) from top side and bottom side for around 5.5 and 5 µm respectively.

ACKNOWLEDGEMENTS

I would like to thank my advisor Prof. Dr. Turgut İKİZ for his support, suggestions and help. I would like to thank Juror, Prof. Dr. Bekir ÖZÇELİK and Ast. Prof. Dr. Şule ÇOLAK for their supports and valuable knowledge. I would like to thank my husband Dr. Onur NANE for his endless support. On the other side, especially I would like to thank to my family. I could not have completed this thesis without their support.

CONTENTS **PAGE**

LIST OF TABLES **PAGE**

LIST OF FIGURES **PAGE**

ABREVIATIONS

E	: Electric field intensity
D	: Electric flux density
H	: Magnetic field intensity
B	: Magnetic flux density
J	: Electric current density
e_0	: Permittivity of free space
m_0	: Permeability of free space
e	: Permittivity
e_r	: Relative dielectric constant
μ	: Permeability
μ_r	: Relative permeability constant
s	: Electric conductivity
Z_0	: Free space impedance
n	: Refractive index
ρ_V	: Volume charge density
ρ_S	: Surface charge density
c	: Light velocity
ω	: Angular frequency
k	: Wave vector
ϕ	: Phase of electromagnetic wave
Γ	: Reflection coefficient
T	: Transmission coefficient
S	: Poynting vector
f	: Frequency

1. INTRODUCTION

The innovations on information and communication technologies have changed many things in human life. The importance of semiconductor components, integrated circuits and devices has been better understood with the development of human society and technology. The performances of integrated circuits such as microprocessors are now well-suited to the famous Moore's law (Moore, 1975), suggests the electronic devices double in speed and capability about every two years. Although, the integrations of electronic components and devices for information communication and processing are approaching the basic speed and bandwidth limit due to ultra-intensive electrical interconnections. In addition to this, electronics industry has faced another problem, size limit. As a fundamental unit, transistors drive most of electronic parts. When we make the transistors smaller, we can also make them faster and consume less electricity to operate. The problem is: how small can we make transistors? At the moment, companies like Intel are producing silicon transistors with 14 nanometer sizes. They are getting very close to the limit of how small we can make a transistor, because of silicon’s 0.2 nm atomic size.

All electronic gadgets like transistors use electrical signals made of electrons moving from one place to another one for communication. Use of light instead of electricity has been considered to be one of the most promising solutions to make electronic components even faster. The main advantage of light is the fastest thing you can use to process and transfer information. Already, fiber optic cables, which simply guide light, are used in current telecommunication technologies.

In recent years, there is widespread research interest in optoelectronics made of optical systems and devices. This area is also called as Photonics, which is a collaborative area of electrical and electronics engineering, material science, physics, and optics. At present, optical integrated circuits using light propagation are being studied and developing intensively. To develop the light based electronic components and devices, it is necessary to create the useful optical materials by giving us a chance to controlling of wave propagation.

Photonic crystals, firstly introduced by Yablonovitch (Yablonovitch, 1987) and John (John, 1987), opened the new fields in application of optoelectronics. Photonic crystals are defined as a periodic composition of dielectric or metallic materials that are designed to control and manipulate of electromagnetic waves. Photonic crystals are attracting more attention day by day due to their intrinsic electromagnetic properties and possible applications in optical devices.

This thesis focuses on the investigation of asymmetric transmission properties of novel dual metallic photonic crystals. The method used in this thesis is FDTD method. The outline of this thesis is as fallows. In this chapter, an introduction to some basics of photonic crystals, optoelectronics, and applications of photonic crystal in optoelectronics is given. Chapter 2 describes the fundamental concepts of our work. The method of analysis we used and problem definition are explained in chapter 3. Numerical results of TM mode analysis obtained by MEEP software and MATLAB are presented in chapter 4. Chapter 5 contains conclusion and scope of future work.

1.1. Photonic Crystals

Photonic crystal is the structure of a periodicity of regularly shaped different dielectric or metallic materials. By the periodicity of dielectric, the transmission of electromagnetic waves is zero at certain frequencies known as the photonic band gap (Ge, 2011). Researchers can be design and construct a photonic crystal with photonic band gaps, which block the wave propagation in certain directions with certain value of wavelengths (certain range of frequency). By creating imperfections (line defects or dot defects, or both) in periodicity of crystal structure, the integrity of the photonic band gap can be broken, which allows manipulating of electromagnetic waves. The localization of electromagnetic wave in photonic band gap allows to design photonic crystal based optical devices (Passaro, 2013).

Electromagnetic wave propagation in the dielectric periodicity was first investigated by Lord Rayleigh (Rayleigh, 1888). The structures were 1-D photonic crystals which have a photonic band gap that prevents electromagnetic wave propagation in plane. Although a single form of photonic crystals has been worked on since 1887, the term "photonic crystal" has begun to be used 100 years after the first discovery, after the publications of Yablonovitch (Yablonovitch, 1987) and John (John, 1987) considered milestones. Before Lord Rayleigh's first study in 1888, the systems with a 1-D photonic band gap which have a broad reflection spectrum were known as stop bands. Further, 1-D photonic crystals which have a multilayer dielectric like Bragg mirror are investigated intensively. Nowadays, certain photonic crystals are applied in a variety of technological practices such as reflecting surface coating for improving the performance of light emitting diodes (LED) and high reflecting mirrors of laser systems. In 1987, Yablonovitch and John have suggested 2-D photonic crystals and 3-D photonic crystals, which have a dielectric periodicity in two-dimensions and three-dimensions, respectively. A1-D photonic band gap results from a 1-D periodic dielectric structure. But both of Yablonovitch's and John's suggestions are interested in2-D and 3-D periodic optical structures. Yablonovitch studied on controlling of photonic density states, for the purpose of operating the diffusion mechanism of compounds inside the photonic crystal. Similarly, John's idea is to influence the control and localization of the electromagnetic wave propagation in the periodic photonic crystal structure. Both of them are concerned with the engineering of a structured material that shows the frequency ranges at which electromagnetic propagation is blocked; namely, photonic band gaps. After the work of 1987, research on photonic crystals led to a serious increase in the number of investigations. However, as a result of the difficulties in producing photonic crystals in the optical dimensions, the first investigations are theoretical studies in the optical and microwave regime where the photonic crystals are much easier to produce at the nanoscale. Yablonovitch has reported the first 3-D photonic band gap for microwave propagation (Yablonovitch, 1991). Thomas Krauss studied on 2-D photonic crystal and reported first demonstration of 2-D photonic crystal in optical regime (Krauss, 1996). His study allowed the production of photonic crystals by the manufacturing techniques used in the semiconductor industry. Even if some methods are used to mature into possible applications, 2-D photonic crystals are commercially available as optical components and fiber optics. Since 1998, the 2-D photonic crystals based optical components such as optical filters (Ma, 2011: Mohmoud, 2012), multiplexers (Rawal, 2009) demultiplexers (Benisty, 2010), switches (Wang, 2010), directional couplers (Moghaddam, 2010), power dividers/splitters (Gannat, 2009), sensors (Malek, 2011: Olyaee, 2012) are studied for possible applications in electronic industry (Passaro, 2013).

The three types of photonic crystal structures can be distinguished according to the change of the refractive index and the periodicity in the medium. These three structure, one-dimensional (1D), two-dimensional (2D) and three-dimensional (3D) as shown in Figure 1.1 respectively.

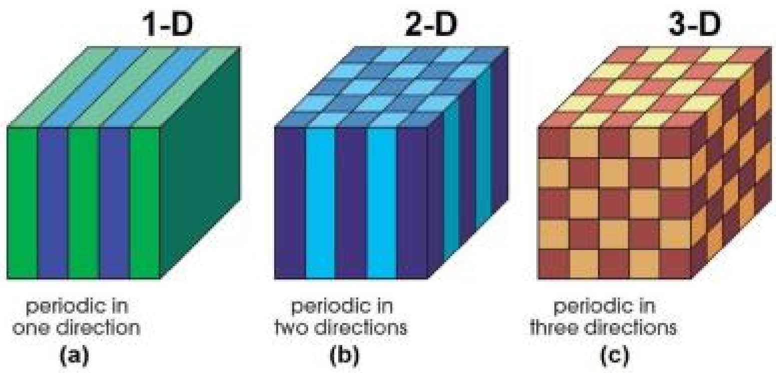

Figure 1.1. Demonstrations of photonic structures in a) 1-D b) 2-D and c) 3-D. The different colors represent materials with different dielectric constant (Joannopoulos, 2008)

In 1-D photonic crystals, the periodic modulation of the refractive index occurs only in one dimension, while the refractive index variations are the same in the other two dimensions of the crystal. The photonic band gap appears in the direction of periodicity for any value of refractive index contrast i.e., difference between the dielectric constants of the materials. Namely, there is no threshold for dielectric contrast for the photonic band gap appearance. The wideness of photonic band gap appears very small where index contrast has small value and vice versa. However, when refractive index contrast has values bigger than one, the photonic band gaps are opened up ($n_1/n_2 > 1$), where n_1 and n_2 are the refractive index of the dielectric materials. A defect can be introduced in a 1-D photonic crystal, by making one of the layers to have a slightly different refractive index or width than the rest. The defect mode is then localized in one dimension however it is extended into other two dimensions. A well known example of this type of 1-D photonic crystal is the Bragg mirror made of variable stages with low and high refractive indices, as shown in Figure 1.1(a) and 1.2(a).

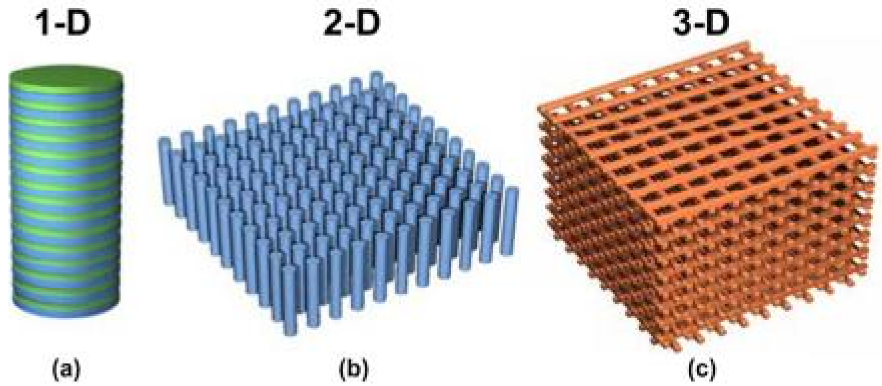

Figure 1.2. Schematic illustrations of photonic crystals (a) 1-D (b) 2-D and (c) 3-D (Passaro, 2013)

The wavelength choosing and reflectivity properties for 1-D photonic crystals are used in a wide range of applications, including high-reflection mirrors (Bruyant, 2003: Li, 2011), optical filters (Chen, 2003: Nemec, 2004: Lee, 2005), waveguides (Taniyama, 2002), and lasers (Lu, 2011). In addition, such 1-D photonic crystals are widely used as antireflective coatings, which significantly reduce surface reflection and are used to enhance the quality of the lenses, prisms and other optical components.

Photonic crystal structures which have a periodicity in two different dimensions and homogeneity in other dimension are known as 2-D photonic crystal shown in Figure 1.1(b) and 1.2(b). In most of the 2-D photonic crystals, the photonic band gap occurs when the lattice has sufficiently larger index contrast. If the refractive index contrast between the cylindrical (or rectangular) rods and the air holes is adequately large, 2-D photonic band gap can occur for electromagnetic wave propagation in the plane of periodicity perpendicular to the rod axis. In general, 2-D photonic band gaps consist of dielectric rods in air host (high dielectric columns positioned in a low dielectric media) or air holes in a dielectric region (low dielectric columns in high dielectric media) as shown in Figures 1.3(a) and 1.3(b). The dielectric rods in air host give photonic band gap in TM mode where the electric field is polarized perpendicular to the plane of periodic dielectrics. The air holes in a dielectric region give TE modes where magnetic field is polarized perpendicular to the plane of periodic dielectrics.

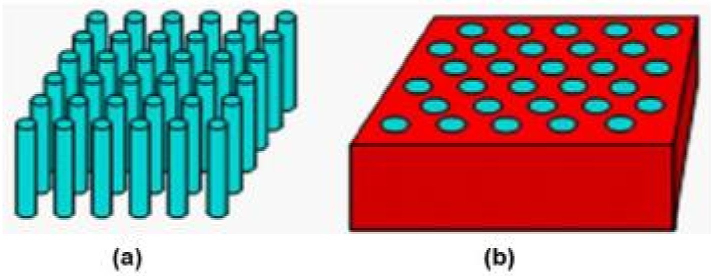

Figure 1.3. Structure of (a) dielectric rods in air and (b) air holes in dielectric region (Passaro, 2013)

A 3-D photonic crystal has a dielectric structure with periodic permeability modulation along three dimensions, provided that the conditions of sufficiently high dielectric contrast and suitable periodicity are met; a photonic band gap appears in all directions. Such 3-D photonic band gaps, unlike the 1-D and 2-D ones, can reflect electromagnetic waves incident from any direction. An example, shown in Figure 1.2(c) depicts the 3-D woodpile structure.

In consequence of difficulties in producing high quality structures for optical wavelengths, early photonic crystals are performed at microwave and mid-infrared frequencies (Ogawa, 2002: Yang, 2009). The smaller photonic structures have become feasible with the developments of methods used in manufacturing and materials processing, and in 1999 the first 3-D photonic crystal with a photonic band gap at communications frequencies is reported (Deubel, 2004: Baohua, 2009). Since then, various lattice geometries have been reported for operation at similar frequencies (Ohkubo, 2004: Liu, 2008). Waveguide and the introduction of intentional defects in 3-D photonic crystals has not progressed as rapidly as in 2-D photonic crystals, due to the fabrication difficulties and the more complex geometry required to achieve 3-D photonic band gaps.

1.2. Optoelectronics

Optoelectronics is a branch of electronic that combines both electronics and optics. Optoelectronic devices are used in various applications in technologies of telecommunication, defense, medical and automation. In this field, the researches focus on developing electronic devices that interact with light forms of ultraviolet, visible and infrared. Optoelectronic devices operate by using photons that can propagate in a dielectric medium. A photon is the elementary unit of light. Photons propagate with a classified frequency such as optical, infrared, microwave and so forth. The relationship between an electromagnetic wave's frequency and its velocity (ν) is given by: $\lambda = \nu / f$ (λ is wavelength). An electromagnetic wave propagates in free space with velocity of 3.0×10^8 m/s. But it propagates slower than free space velocity in other media, such as solids. The use of photons instead of electrons in integrated circuits is summarized in the following explanatory table.

Table 1.1. Summary of using photons instead of electron in Integrated Circuit Technology.

Features	In Electronic	In Photonic
Data Carrier	electrons	photons
Type of Components	transistors	functional optical devices
Number of Components Integrated	limited to a few hundred	range into millions
Substrate Materials	many different materials in a single chip	fits nicely onto silicon

In recent years, the use of photonic crystals in production of optoelectronic devices is considered as the most innovative approach. The studies on optoelectronic, have demonstrated progress toward photonic crystal based integrated circuits. The compatibility of new and faster light based chips with all the existing electronic chips is considered as a key challenge.

1.3. Usage of 2-D Photonic Crystals in Optoelectronics

The ability of controlling and manipulating of the electromagnetic propagation by dielectric periodicity in photonic crystals, and related formation of photonic band gap can be used for designing of the optoelectronic devices. At present, pioneering improvements in optoelectronic devices have greatly benefited lighting and display technologies. Nevertheless, 2-D photonic crystal which is very useful type of photonic band gap material and can block light from traveling within a plane is the choice of great interest for both fundamental and applied research, and also it is beginning to find commercial applications. K. Inoue (Inoue, 2004) has summarized the use of photonic crystals in several applications given in figure 1.4.

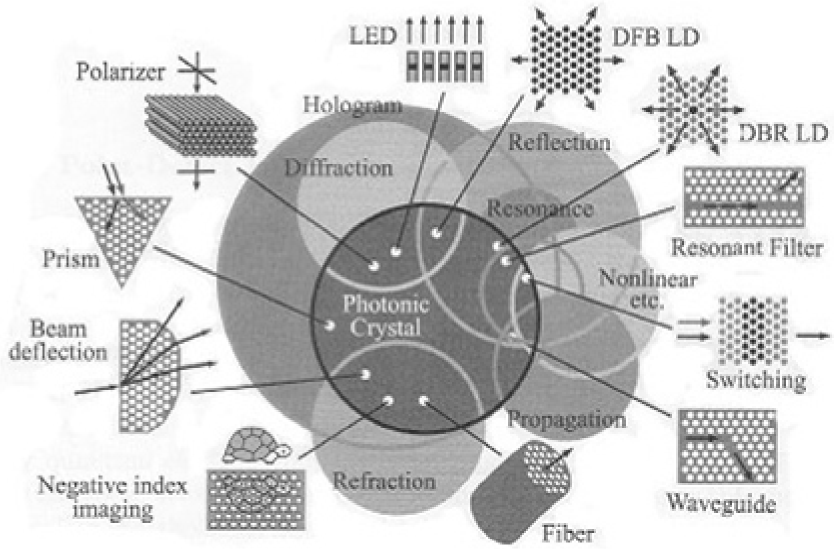

Figure 1.4. Samples of photonic crystals applications (Inoue, 2004)

The majority of photonic crystal applications utilize the phenomenon of photonic band gap that opens the new routes to design optical components in micrometer (μm) range. Waveguides that confine light via photonic band gaps are a new development. In general, the waveguide is designed to transmit electromagnetic propagation of a particular frequency from one place to another place on a curved path. Many studies on optical components using this waveguide have been reported in the literature such as power splitter/ power divider (Djavid,2008) equally between output waveguides, Y splitter (Borel, 2005), directional couplers (Moghaddam, 2010), optical diode (Scalora, 1994) and so on. It is also possible to design a cavity, formed by the absence of a single rod or group of rods (dot defects), which is embedded between two waveguides each of which is formed by the absence of a row of rods (line defects).

2. FUNDAMENTAL CONCEPTS

2.1. Maxwell's Equations

Electromagnetic wave phenomenon can be explained by Maxwell's equations depending on both space and time. They were established by James Clerk Maxwell in 1873 as a compilation of empirically observed laws previously shown to describe the behavior of electric and magnetic fields (Maxwell, 1954). They consist of Ampere's law (Ampere, 1820), Faraday's law (Faraday, 1834), and Gauss' law (Gauss, 1839). The differential form Maxwell's equations as fallows;

$$\nabla \times \mathbf{E} = -\frac{\delta \mathbf{B}}{\delta \mathrm{t}} \quad (2.1)$$

$$\nabla \times \mathbf{H} = \mathbf{J} + \frac{\delta \mathbf{D}}{\delta \mathrm{t}} \quad (2.2)$$

$$\nabla \cdot \mathbf{D} = \rho_V \quad (2.3)$$

$$\nabla \cdot \mathbf{B} = 0 \quad (2.4)$$

Maxwell's contribution to these laws is the addition of the displacement current term (the term involving the time derivative) in Ampere's law. These equations can be greatly simplified if a few reasonable assumptions are made. **E** and **D**, and **H** and **B** are related by the constitutive relations

$$\mathbf{D} = e\mathbf{E} \quad (2.5)$$

$$\mathbf{B} = \mu\mathbf{H} \quad (2.6)$$

$$\mathbf{J} = s\mathbf{E} \quad (2.7)$$

here $e = e_0 e_r$ is the dielectric permittivity, $\mu = \mu_0\mu_r$ is permeability, e_r is the relative dielectric constant, and s is electric conductivity. For now, we can count $\mu_r = 1$. Firstly, let's consider two theorems of Stokes's and Gauss's

$$\oint_S \mathbf{F} \cdot \mathrm{ds} = \int_V \nabla \cdot \mathbf{F}\mathrm{dv} \quad (2.8)$$

here s is the closed surface area defining volume V. The Stokes theorem is as fallowing

$$\oint_C \mathbf{F} \cdot \mathrm{dl} = \int_A \nabla \times \mathbf{F} \cdot \mathrm{ds} \quad (2.9)$$

here contour C defines surface area A. We can transform the Maxwell's equations in differential form to integral one with the above theorems. Maxwell's equations in Integral forms are

$$\oint_S \mathbf{D} \cdot \mathrm{ds} = \int_V \rho_V \mathrm{dv} \quad (2.10)$$

$$\oint_S \mathbf{B} \cdot \mathrm{ds} = 0 \quad (2.11)$$

$$\oint_L \mathbf{E} \cdot \mathrm{dl} = -\int_A \frac{\partial \mathbf{B}}{\partial t} \quad (2.12)$$

$$\oint_L \mathbf{H} \cdot \mathrm{dl} = \int_A \frac{\partial \mathbf{D}}{\partial t} + I \quad (2.13)$$

The characteristics of the medium are usually defined by μ, e, and s. Moreover, the main role for the dielectric media is played by e. The dielectric media is called as linear when e is not function of **E**; in other case it is nonlinear. If it is independent from the location in space, it is called as homogeneous; versa inhomogeneous. If intrinsic parameters are not function of distance, the medium is isotropic; versa anisotropic.

2.2. Wave Equation

When we assume $\mathbf{J}$ = 0 and ρ_V= 0, the wave equation can be rewritten by executing ∇x operator to both sides of equation (2.1)

$$\nabla \times \nabla \times \mathbf{E} = -\frac{\partial}{\partial t}(\nabla \times \mathbf{B}) = -\mu\frac{\partial}{\partial t}(\nabla \times \mathbf{H}) = -\mu\frac{\partial}{\partial t}\frac{\partial \mathbf{D}}{\partial t} = -\mu\varepsilon\frac{\partial^2 \mathbf{E}}{\partial^2 t}$$

By using equation (2.2) and (2.5), then applying the following formula

$$\nabla \times \nabla \times \mathbf{E} = \nabla(\nabla \cdot \mathbf{E}) - \nabla^2 \mathbf{E} \tag{2.14}$$

one finds as fallow with equation (2.3)

$$\nabla^2 \mathbf{E} = \mu\varepsilon\frac{\partial^2}{\partial^2 t}\mathbf{E} \tag{2.15}$$

Equation (2.15) is called as the wave equation. The same method can be applied for the magnetic field. The quantity με gives the speed of electromagnetic wave in space as (assuming μ_r= 1).

$$\mu\varepsilon = \mu_0\varepsilon_0\varepsilon_r = \frac{\check{n}^2}{c^2} \tag{2.16}$$

Here, n is related to the refractive index of media.

2.3. Time-Harmonic Fields

It the fields are arbitrary periodic time functions, they can be explained into Fourier series of harmonic sinusoidal components. In this case the phasor of such a field can be defined as;

$$\mathbf{E}(r,t) = \mathrm{Re}\{\mathbf{E}(r)e^{j\omega t}\} \tag{2.17}$$

Here Re {...} indicates the real part of quantity in brackets and ω is the angular frequency in rad/s. The source-free Maxwell's equations are as followings by using the time-harmonic assumption (2.17)

$$\nabla \times \mathbf{E} = -j\omega\mu\mathbf{H} \quad (2.18)$$

$$\nabla \times \mathbf{H} = j\omega\varepsilon\mathbf{E} \quad (2.19)$$

By same assumption, the wave equation (2.15) can be reduced to:

$$\nabla^2\mathbf{E} + k^2\mathbf{E} = 0 \tag{2.20}$$

Here $k = \omega\sqrt{\mu\varepsilon}$.

By considering of propagating of a uniform plane wave which is characterized by a uniform electric field where E_x is not zero.

$$\frac{\delta^2\mathbf{E}_x}{\delta x^2} = 0,\ \frac{\delta^2\mathbf{E}_x}{\delta y^2} = 0 \tag{2.21}$$

The wave equation becomes

$$\frac{\delta^2 \mathbf{E}_x}{\delta z^2} + k^2 \mathbf{E}_x = 0 \tag{2.22}$$

The solution should be

$$\mathbf{E_x}(z) = E_0 e^{jkz} \tag{2.23}$$

The Maxwell's equation (2.18) gives the magnetic field

$$\nabla \times \mathbf{E} = \begin{vmatrix} a_x & a_y & a_z \\ 0 & 0 & \frac{\partial}{\partial z} \\ \mathbf{E}_x(z) & 0 & 0 \end{vmatrix} = -j \quad \mu\left(a_x \mathbf{H}_x + a_y \mathbf{H}_y + a_z \mathbf{H}_z\right) \tag{2.24}$$

Here a_x, a_y, a_z are unit vectors in Cartesian coordinate. If we use the above expression

$$\mathbf{H}_x = 0 \tag{2.25}$$

$$\mathbf{H}_y = \frac{1}{j\omega\mu} \frac{\partial \mathbf{E}_x(z)}{\partial z}$$

$$\mathbf{H}_z = 0$$

For magnetic field, we can obtain the fallowing equation by using the solution of $E_x(z)$

$$\mathbf{H} = a_{\mathbf{y}} \mathbf{H}_y(z) (2.26)$$

$$= \frac{1}{-j\omega\mu}(-jk\mathbf{E}_x)a_y (2.27)$$

$$= a_y \frac{k}{\omega\mu} \mathbf{E}_x(z)$$

$$= a_y \frac{k}{Z} \mathbf{E}_x(z)$$

Here the medium impedance is defined as $Z = \sqrt{\mu/e}$. The electromagnetic wave propagation is illustrated in figure 2.1.

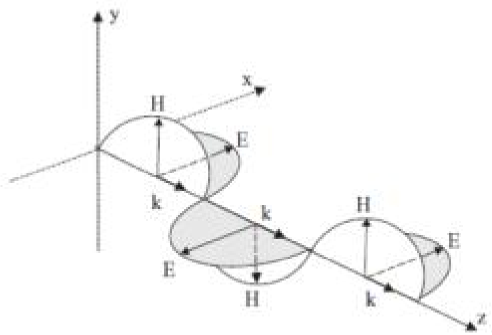

Figure 2.1. Illustration of an electromagnetic wave (Wartak, 2013)

Finally, we have a useful relation between electric and magnetic fields in source-free region. Assuming time-harmonic and plane-wave dependence of electric and magnetic fields as

$$\mathbf{E} \sim \exp(i\omega t - ik \cdot r)$$

We can relate the equation (2.6) and Maxwell equation (2.1) to obtain

$$k \times \mathbf{E} = \omega\mu_0 \mathbf{H}$$

Introducing unit vector $\hat{k}$ along wave vector k and the expression for wave number $k = \omega \check{n} \sqrt{\mu_0 \varepsilon_0}$, we have

$$\check{n}\hat{k} \times \mathbf{E} = Z_0 \mathbf{H}$$

Here Z_0 is the free-space impedance.

2.4. Polarized Waves

Polarization is a property of electromagnetic waves that define the direction of their oscillation. Polarization defines a time-dependent curve which **E** vector makes (in the plane orthogonal to the direction of propagation) in a given space. If the curve has an elliptical shape the wave is known as elliptically polarized. Besides, the ellipse may be reduced to a circle or a segment of a straight line. In this case, the wave is called as circularly or linearly polarized, respectively. Because of the electric and magnetic field vectors are interdependent; they do not need a separate process.

2.4.1. Linearly Polarized Waves

Firstly, we need an equation for an electromagnetic wave which is defined by electric field vector **E** directed along the x-axes

$$\mathbf{E} = a_x \mathbf{E}_0 \cos(\omega t - kz + \phi) \quad (2.28)$$

When the electric field vector is oscillating in x-axes, it is called as a linearly polarized plane wave. The electromagnetic wave propagation is in z-axes. In equation (2.28) k is the propagation constant and ω=2πν is the angular frequency, we have

$$k = \frac{\omega}{v}$$

Here v = c/ň is the speed of the propagation in a media which has the refractive index ň. The parameter ϕ is the phase of wave. The wave equation can be written in complex form as

$$\mathbf{E} = a_x \mathbf{E}_0 e^{i(\omega t - kz + \phi)} \quad (2.29)$$

The electric field which is defined in equation (2.28) is rewritten by taking real part of equation (2.29). Now, we have a general equation for a plane polarized wave

$$\mathbf{E} = \hat{e}\mathbf{E}_0 e^{\,i(\omega t - k \cdot r + \phi)}$$

Here unit vector ê lies in the plane known as plane of polarization. It is perpendicular to vector k which lies in direction of propagation

$$k \cdot \hat{e} = 0$$

2.4.2. Circularly and Elliptical Polarized Waves

Generally, when we have an arbitrary number of plane waves propagating in the same direction they add up to a complicated wave. Basically, one has only two such plane waves. We can consider two linearly polarized plane waves which propagate in orthogonal direction and having the same frequencies

$$\mathbf{E}_1 = \mathbf{E}_x a_x = a_x \mathbf{E}_{0x} \cos(\omega t - kz) \tag{2.30}$$

$$\mathbf{E}_2 = \mathbf{E}_y a_y = a_y \mathbf{E}_{0y} \cos(\omega t - kz + \phi) \tag{2.31}$$

We need to know form of the resulting wave and the curve traced by the tip of the total electric vector $\mathbf{E} = \mathbf{E}_1 + \mathbf{E}_2$

$$\mathbf{E} = \mathbf{E}_1 + \mathbf{E}_2 = E_0\{\cos(\omega t - kz) + \cos(\omega t - kz + \phi)\}$$

From equation (2.30)

$$\cos\,(\omega t\ -\ kz)\ =\ \frac{\mathbf{E}_{x}}{\mathbf{E}_{ox}}(2.32)$$

we have the following trigonometric equality

$$\cos\,(\alpha\ -\ \beta)\ \ =\ \ \cos\alpha\cos\beta\ \ +\ \ \sin\alpha\sin\beta$$

so equation (2.31) can be rewritten as following;

$$\mathbf{E}_{y}\ \ =\ \ \mathbf{E}_{0y}\left\{\cos\,(\omega t\ -\ kz)\cos\delta + [1-\cos^{2}(\omega t\ -\ kz)]^{1/2}\sin\delta\right\}$$

By substituting equation (2.32) into the above equation we can drive

$$\frac{\mathbf{E}_{y}}{\mathbf{E}_{0y}}\ =\frac{\mathbf{E}_{x}}{\mathbf{E}_{0x}}\cos\phi + \left(1-\frac{\mathbf{E}_{0}^{2}}{\mathbf{E}_{0x}^{2}}\right)^{1/2}\sin\phi.$$

Squaring both sides gives

$$\left(\frac{\mathbf{E}_{y}}{\mathbf{E}_{0y}}-\frac{\mathbf{E}_{x}}{\mathbf{E}_{0x}}\cos\phi\right)^{2}\ =\ \left(1-\frac{\mathbf{E}_{0}^{2}}{\mathbf{E}_{0x}^{2}}\right)^{1/2}\sin\phi$$

or

$$\frac{\mathbf{E}_{y}^{2}}{\mathbf{E}_{0y}^{2}}-2\cos\phi\frac{\mathbf{E}_{y}}{\mathbf{E}_{0y}}\frac{\mathbf{E}_{x}}{\mathbf{E}_{0x}}+\frac{\mathbf{E}_{x}^{2}}{\mathbf{E}_{0x}^{2}}\cos^{2}\phi+\frac{\mathbf{E}_{x}^{2}}{\mathbf{E}_{0x}^{2}}\sin^{2}\phi\ =\ \sin^{2}\phi$$

Finally, we obtain

$$\left(\frac{\mathbf{E}_{y}}{\mathbf{E}_{0y}}\right)^{2}+\left(\frac{\mathbf{E}_{x}}{\mathbf{E}_{0x}}\right)^{2}-2\left(\frac{\mathbf{E}_{y}}{\mathbf{E}_{0y}}\right)\left(\frac{\mathbf{E}_{x}}{\mathbf{E}_{0x}}\right)\cos\phi\ =\ \ \sin^{2}\phi(2.33)$$

This equation describes an ellipse. Thus the endpoint of **E** (z, t) traces an elliptical trace. This wave is known as elliptically polarized. For $\phi=\pi/2$, the resultant total electric field is given by

$$\left(\frac{\mathbf{E}_y}{\mathbf{E}_{0y}}\right)^2 + \left(\frac{\mathbf{E}_x}{\mathbf{E}_{0x}}\right)^2 = 1$$

and describes a circular trace if $\mathbf{E}_{0y}=\mathbf{E}_{0z}$.

This means that the end of electric vector **E** of right elliptically polarized wave revolves clockwise around the ellipse. Typical situations of elliptic, circular and linear polarizations are shown in figure 2.2.

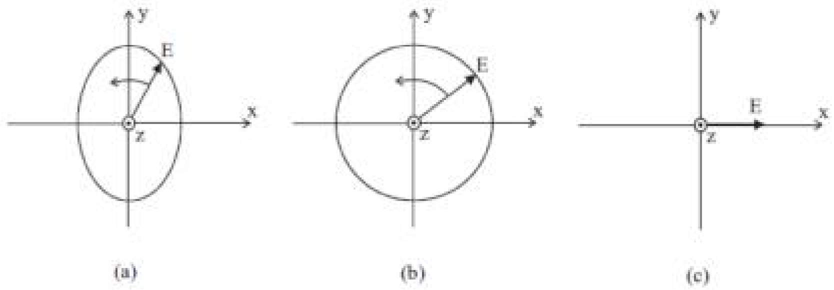

Figure 2.2. Representation of polarization types: (a) elliptical, (b) circularly and (c) linearly (Wartak, 2013)

2.4.3. Fresnel Coefficients and Phases

Consider an electromagnetic wave that reflects at the boundary between two dielectric medium as shown in figure 2.3. The incoming wave plane is described as the plane on which the unit vector n is formed, where unit vector n is normal to the directions of propagation of the reflected and incident waves and the interface between two dielectric media.

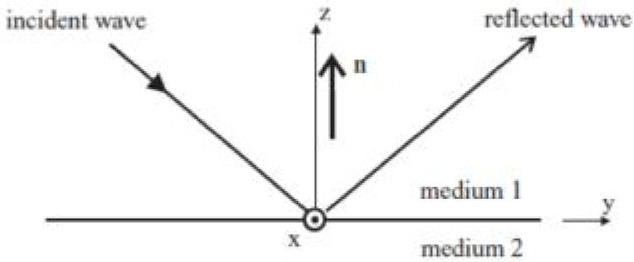

Figure 2.3. Reflection of a wave at the interface (Wartak, 2013)

We can obtain the reflection and transmission coefficients known as Fresnel coefficients which depend on the εdielectric constant and the angle (Popovic, 2000). Also, Fresnel coefficients give Fresnel phases by the following equation (Kraus, 1992):

$$\Gamma = e^{-2j\phi}. \quad (2.34)$$

For modes of TM and TE, the reflection coefficient Γ and phase ϕ can be calculated.

2.4.4. TE Polarization

The incident, reflected and transmitted electric fields are $\mathbf{E}_{1i}$, $\mathbf{E}_{1r}$, $\mathbf{E}_{2t}$, respectively and shown in figure 2.4. The incident electric field $\mathbf{E}_{1i}$is parallel to the interface between two media. This orientation is called as TE polarization. In general, the electric field vector **E** is normal to the plane of incidence.

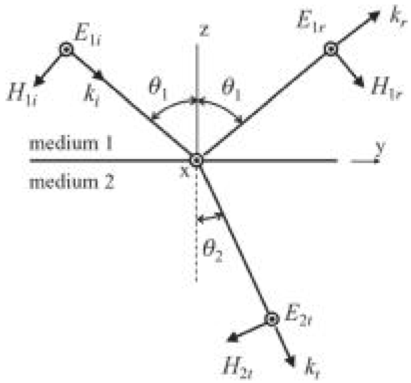

Figure 2.4. The incident, reflected and transmitted components of electric and magnetic fields for TE polarization (Wartak, 2013)

The sum of the components on both sides must be equal by the boundary conditions. These conditions give

$$\mathbf{E}_{1i} + \mathbf{E}_{1r} = \mathbf{E}_{2t} \tag{2.35}$$

$$-\mathbf{H}_{1i}\cos\theta_1 + \mathbf{H}_{1r}\cos\theta_1 = -\mathbf{H}_{2t}\cos\theta_2$$

We also have the following equations including the impedances in two medium:

$$\frac{\mathbf{E}_{1i}}{\mathbf{H}_{1i}} = Z_1, \ \frac{\mathbf{E}_{1r}}{\mathbf{H}_{1r}} = Z_1, \ \frac{\mathbf{E}_{2t}}{\mathbf{H}_{2t}} = Z_2 \tag{2.36}$$

The impedance Z is equal to Z_0/ň for a nonmagnetic medium ($\mu_r = 1$), where ň is the refractive index of the medium, where Z_0 is the intrinsic impedance of the free-space given by

$$Z_0 = \sqrt{\frac{\mu_0}{\varepsilon_0}}$$

The above equation defines the impedance of the free space. By using the second part of equation (2.35) and the equation (2.36), we have

$$\mathbf{E}_{1i} + \mathbf{E}_{1r} = \mathbf{E}_{2t}$$

$$-\frac{\mathbf{E}_{1i}}{\mathbf{Z}_1}\cos\theta_1 + \frac{\mathbf{E}_{1r}}{\mathbf{Z}_1}\cos\theta_1 = -\frac{\mathbf{E}_{2t}}{\mathbf{Z}_2}\cos\theta_1.$$

Reflectance coefficient is defined as

$$\Gamma_{TE} = \frac{\mathbf{E}_{1r}}{\mathbf{E}_{1i}} \tag{2.37}$$

We can use equations (2.47) and (2.48), to get

$$\Gamma_{TE} = \frac{Z_2\cos\theta_1 - Z_1\cos\theta_2}{Z_2\cos\theta_1 + Z_1\cos\theta_2}$$

By changing the impedance values by refractive indices ň, last expression is

$$\Gamma_{TE} = \frac{\check{n}_1\cos\theta_1 - \check{n}_2\cos\theta_2}{\check{n}_1\cos\theta_1 + \check{n}_2\cos\theta_2}$$

This equation can be simplified by using Snell's law

$$\Gamma_{TE} = \frac{\check{n}_1\cos\theta_1 - \check{n}_1\frac{\sin\theta_1}{\sin\theta_2}\cos\theta_2}{\check{n}_1\cos\theta_1 + \check{n}_1\frac{\sin\theta_1}{\sin\theta_2}\cos\theta_2} = \frac{\cos\theta_1\sin\theta_2 - \sin\theta_1\cos\theta_2}{\cos\theta_1\sin\theta_2 + \sin\theta_1\cos\theta_2} \tag{2.38}$$

In this case, Γ_{TE} reduces to the simple form

$$\Gamma_{TE} = \frac{\cos\theta_1\sin\theta_2 - \sin\theta_1\cos\theta_2}{\cos\theta_1\sin\theta_2 + \sin\theta_1\cos\theta_2} = \frac{\sin(\theta_1-\theta_2)}{\sin(\theta_1+\theta_2)} \equiv \frac{a-jb}{a+jb}$$

We can write Γ_{TE} as a complex number as

$$\Gamma_{TE} = \frac{e^{-j\phi_{TE}}}{e^{j\phi_{TE}}} = e^{-2j\phi_{TE}}$$

Finally, by principle of Fresnel, equation (2.34) one phase is obtained as

$$\tan\phi_{TE} = \frac{\sqrt{\check{n}_1^2\sin^2\theta_1 - \check{n}_2^2}}{\check{n}_1\cos\theta_1} \quad (2.39)$$

This expression describes the phase shift for the reflected wave in TE mode. The reflection coefficient (Pedrotti, 2007) is defined as

$$\Gamma = \left(\frac{\check{n}_1-\check{n}_2}{\check{n}_1+\check{n}_2}\right)^2 \qquad (2.40)$$

2.4.5. TM Polarization

We can analyze the reflection for TM polarization where electric field vector **E** is parallel to the plane of incidence and the magnetic field is parallel to the interface between two mediums shown in figure 2.5.

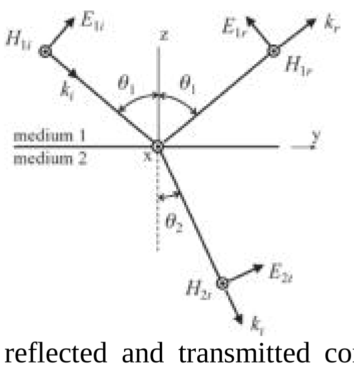

Figure 2.5. The incident, reflected and transmitted components of electric and magnetic fields for TM polarization (Wartak, 2013)

We can obtain the reflection coefficient r_{TM} for the TM mode by using the $\mathbf{E}_{1i}$, $\mathbf{E}_{1r}$, $\mathbf{E}_{2t}$ which are complex values of incident, reflected and transmitted electric fields in two different dielectric media respectively. Same notation is used for components of magnetic field. The sum of the components on both sides must be equal according to the boundary conditions. These conditions give

$$\mathbf{E}_{1i}\cos\theta_1 - \mathbf{E}_{1r}\cos\theta_1 = \mathbf{E}_{2t}\cos\theta_2 \qquad (2.41)$$

$$\mathbf{H}_{1i} + \mathbf{H}_{1r} = \mathbf{H}_{2t}$$

Using equation (2.36) for Z to terminate the expressions of the magnetic part from the above equation (2.41). Now we have

$$\mathbf{E}_{1i}\cos\theta_1 - \mathbf{E}_{1r}\cos\theta_1 = \mathbf{E}_{2t}\cos\theta_2 \qquad (2.42)$$

$$\frac{\mathbf{E}_{1i}}{\mathbf{Z}_1} + \frac{\mathbf{E}_{1r}}{\mathbf{Z}_1} = \frac{\mathbf{E}_{2t}}{\mathbf{Z}_2}$$

Reflection coefficient is obtained as

$$\Gamma_{TM} = \frac{\mathbf{E}_{1r}}{\mathbf{E}_{1i}} \qquad (2.43)$$

using equation (2.42)

$$\Gamma_{TM} = \frac{Z_1\cos\theta_1 - Z_2\cos\theta_2}{Z_1\cos\theta_1 + Z_2\cos\theta_2}$$

This equation can be rewritten by using the refractive index parameter

$$\Gamma_{TM} = \frac{\check{n}_2\cos\theta_1-\check{n}_1\cos\theta_2}{\check{n}_2\cos\theta_1+\check{n}_1\cos\theta_2}$$

or

$$= \frac{\check{n}_2\cos\theta_1-\sqrt{\check{n}_1^2-\check{n}_2^2\cos\theta_1}}{\check{n}_2\cos\theta_1+\sqrt{\check{n}_1^2-\check{n}_2^2\cos\theta_1}} \quad (2.44)$$

Finally, we have a phase equation for TM mode as following. This equation has the same notation as for TE mode.

$$\tan\phi_{TE} = \frac{\check{n}_1^2}{\check{n}_2^2} \times \frac{\sqrt{\check{n}_1^2\sin^2\theta_1-\check{n}_2^2}}{\check{n}_1\cos\theta_1} \quad (2.45)$$

2.5. Poynting Theorem

When an electromagnetic wave propagates in a dielectric medium, it carries some electromagnetic energy. The electromagnetic energies associated by the wave can be described via Poynting theorem. By using the equations (2.1) and (2.2)

$$\nabla \times \mathbf{E} = -\frac{\delta\mathbf{B}}{\delta t}$$

$$\nabla \times \mathbf{H} = \mathbf{J} + \frac{\delta\mathbf{D}}{\delta t}$$

We have the following equation

$$\nabla \cdot (\mathbf{E} \times \mathbf{H}) = \mathbf{H} \cdot (\nabla \times \mathbf{E}) - \mathbf{E}(\nabla \times \mathbf{H}). \quad (2.46)$$

By using equations (2.1) and (2.2) , the equation (2.46) is rewritten as

$$\nabla \cdot (\mathbf{E} \times \mathbf{H}) = -\mathbf{H} \cdot \mu \frac{\delta \mathbf{H}}{\delta \mathrm{t}} - \mathbf{E} \cdot \mathbf{J} - \mathbf{E} \cdot \mu \frac{\delta \mathbf{E}}{\delta \mathrm{t}}$$

$$= -\mu \frac{1}{2} \frac{\delta \mathbf{H} \cdot \mathbf{H}}{\delta \mathrm{t}} - \sigma \mathbf{E}^2 - \varepsilon \frac{1}{2} \frac{\delta \mathbf{E} \cdot \mathbf{E}}{\delta \mathrm{t}}$$

$$= -\frac{\partial}{\partial \mathrm{t}} \left(\frac{1}{2} \varepsilon \mathbf{E}^2 + \frac{1}{2} \mu \mathbf{H}^2 \right) - \sigma \mathbf{E}^2 \quad (2.47)$$

integrating both sides of the equation (2.47) and applying the Gauss’s theorem, we can get,

$$\int_V \nabla \cdot (\mathbf{E} \times \mathbf{H}) \mathrm{dv} = -\frac{\partial}{\partial t} \int_V \left(\frac{1}{2} \varepsilon \mathbf{E}^2 + \frac{1}{2} \mu \mathbf{H}^2 \right) \mathrm{dv} - \int_V \sigma \mathbf{E}^2 \mathrm{dv}$$

(2.48)

The Poynting vector S is obtained as following

$$\mathbf{S} = \mathbf{E} \times \mathbf{H} \quad (2.49)$$

Equation (2.48) can be expressed as,

$$-\oint_S S \cdot ds = \frac{\partial}{\partial t} \int_V (\ _{e} + \ _{m}) \mathrm{dv} + \int_V \mathrm{p_o} \mathrm{dv} \quad (2.50)$$

Here

$\mathrm{p_o} = \sigma \mathbf{E}^2$ is ohmic power density

$\ _{m} = \frac{1}{2} \mu \mathbf{H}^2$ is magnetic energy density

$\ _{e} = \frac{1}{2} \varepsilon \mathbf{E}^2$ is electric energy density.

3. NUMERICAL METHOD

In this thesis, we investigated asymmetric transmission properties of two dimensional metallic gratings for optoelectronic applications. We tried to obtain asymmetric propagation behavior by changing the geometry of metallic grating. According to reference paper (M. Stolarek, 2013: Cheng, 2007: Cheng, 2008: Xu, 2011), we have considered some dual metal geometries and studied the transmission spectrum of these structures by freely available MEEP program (MIT Electromagnetic Equation Propagation). We have also compared the MEEP's simulation results by MATLAB. We will use FDTD method in our study. Meep implements the FDTD method for computational electromagnetism. FDTD algorithm is today's most popular calculation tools (Taflove, 2000). The time and space are divided in a uniform grid for FDTD algorithm which solves time dependent Maxwell equations. For determination of boundary conditions, Perfect matched layer (PML) is embedded in the simulation (Berenger, 1994). Generally, the width of PML layer is equal to a lattice constant in overall simulation area. FDTD solves time-space dependent magnetic and electric fields in different spatial regions by sliding electric and magnetic field components. This idea of grid discretization was first proposed by Yee (Yee, 1966). Fields in grids can be classified as TM and TE polarization.

3.1. Finite Difference Time Domain Method (FDTD)

There are many approaches to numerical solution of electromagnetic problems; the popular one of them is the FDTD method. It is widely used in the analysis of antennas, dielectrics, microstrip circuits, scattering from different objects, electromagnetic absorption in the human body exposed to radiation, and photonic crystals (PhC). Since the date of first reported by K. Yee (Yee, 1966), the method has been developed by many researchers. In this method, structure is composed to grid which is discretized in space and time as shown in Figure 3.2.

Derivatives in Maxwell's equations are defined in terms of finite differences on the grid points. By solving the difference equations, update equations which are used for determining the unknown future field values in terms of the past field are obtained. Then the EM field distribution and interaction with structure are revealed.

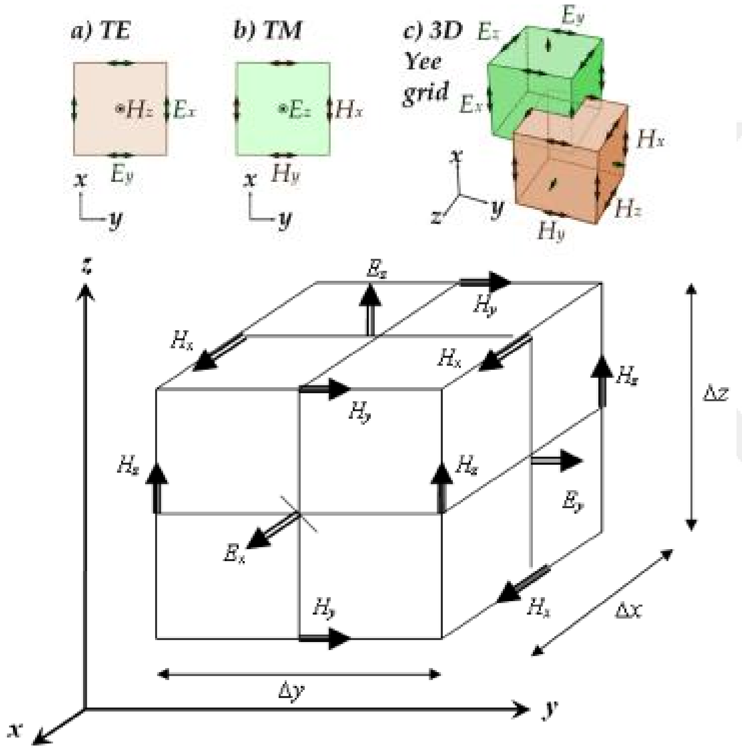

Figure 3.1. The position of the Yee space cage of the electric and magnetic fields in a unit cell.

When d=dx=dy=dz and dt are indicated to increase of space and time respectively, the finite difference derivatives are as follows (Allen, 2005: Taflove 1974).

$$\frac{dF^n(i,j,k)}{d} = \frac{F^n\left(i+\frac{1}{2},j,k\right)-F^n\left(i-\frac{1}{2},j,k\right)}{d} + O(d^2) \tag{3.1}$$

$$\frac{dF^n(i,j,k)}{dt} = \frac{F^{n+1/2}(i,j,k)-F^{n-1/2}(i,j,k)}{dt} + O(dt^2) \qquad (3.2)$$

Here, the statement shown in brackets with *O* is the amount of error in this method. If the distance between two points taken derivative is small enough that all the terms represented by *O* are negligible.

TM and TE modes components are taken as (**E**z, **H**x, **H**y) and (**H**z, **E**x, **E**y) for two dimensional structure respectively. Applying the difference Equations (3.1) and (3.2) to Maxwell's equation, following equations are obtained for TM mode.

$$\mathbf{E}_z^{n+1/2}(i,j) = \mathbf{E}_z^{n-1/2}(i,j) + \frac{cdt}{\varepsilon(i,j)dx}\left[\mathbf{H}_y^n\left(i+\frac{1}{2},j\right) - \mathbf{H}_y^n\left(i-\frac{1}{2},j\right)\right] - \frac{cdt}{\varepsilon(i,j)dy}\left[\mathbf{H}_x^n\left(i,j+\frac{1}{2}\right) - \mathbf{H}_x^n\left(i,j-\frac{1}{2}\right)\right] \qquad (3.3)$$

$$\mathbf{H}_x^{n+1}\left(i,j+\frac{1}{2}\right) = \mathbf{H}_x^n\left(i,j+\frac{1}{2}\right) + \frac{cdt}{\mu\left(i,j+\frac{1}{2}\right)dy}\left[\mathbf{E}_z^{n+\frac{1}{2}}(i,j) - \mathbf{E}_z^{n+\frac{1}{2}}(i,j+1)\right] \qquad (3.4)$$

$$\mathbf{H}_y^{n+1}\left(i+\frac{1}{2},j\right) = \mathbf{H}_y^n\left(i+\frac{1}{2},j\right) + \frac{cdt}{\mu\left(i+\frac{1}{2},j\right)dx}\left[\mathbf{E}_z^{n+\frac{1}{2}}(i+1,j) - \mathbf{E}_z^{n+\frac{1}{2}}(i,j)\right] \qquad (3.5)$$

Solving the Equations (3.3), (3.4) and (3.5) numerically for each lattice point with beginning from initial values to the next point, time domain analysis of photonic crystal can be performed. To keep the stability, following Courant condition must be satisfied for time and space.

$$v_{max}dt \le \left(\frac{1}{dx^2} + \frac{1}{dy^2} + \frac{1}{dz^2}\right)^{-\frac{1}{2}} \qquad (3.6)$$

Besides, to prevent the reflection from the lattice ends, perfectly matched layer (PML) should be placed around the structure (Berenger, 1994).

3.2. Geometry of Problem

Figure 3.3 illustrates scheme of the simulation setup for the investigation of the asymmetry of light transmission of our designs made by dual metal grating. The unidirectional transmittances of terahertz wave's incidence from top side and bottom side were obtained in TM mode. In this simulation, we use perfectly matched layer (PML) (Berenger, 1994) boundary conditions which absorbs electromagnetic waves at the boundaries without reflections. Here, interference waves are sinusoidal wave. The dual metal structures were embedded in free space (ϵ=μ=1) surrounded by PML. The MEEP simulation results were also checked with snapshots of wave propagation obtained by MATLAB for same design structures. Procedure of FDTD and calculating transmittance was provided as below. The size of metal gratings chosen for different designs will be given in result section.

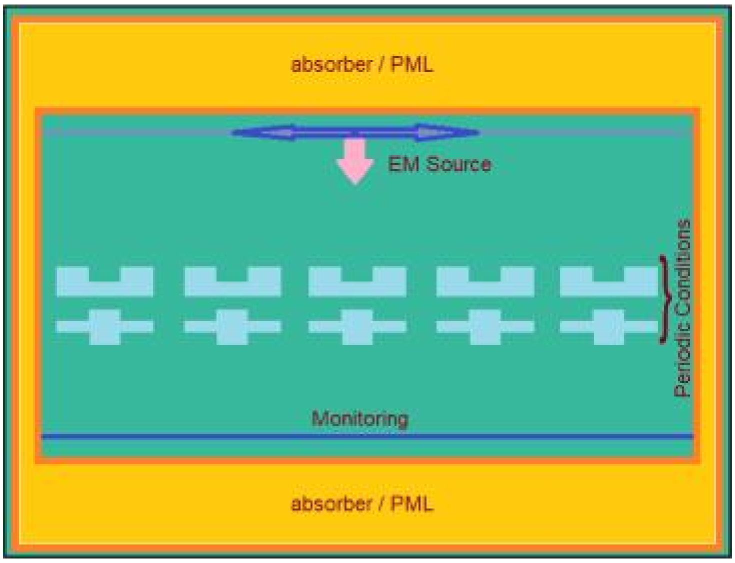

Figure 3.2. FDTD Simulation setup with perfectly matched layer (PML).

Procedure of Calculating Transmission and Reflection Coefficients

3. Performing FDTD based simulation
   b. Calculating the steady state field in the region where reflection and transmission are observed
4. For selected frequency
   f. Calculating the wave vector components of the spatial harmonics
   g. Calculating the complex amplitude of the spatial harmonics
   h. Calculating the diffraction efficiency of the spatial harmonics
   i. Calculating over all reflection and transmission coefficient
   j. Calculating conservation of energy

Procedure for FDTD

1. Simulate the device using FDTD and calculate the steady-state field at reflection and transmission record planes.

$$\mathbf{E}_{\mathrm{ref}}\,(\,x, f\,),\;\; \mathbf{E}_{\mathrm{trn}}\,(\,x, f\,),\;\; \mathbf{E}_{\mathrm{src}}\,(\,x, f\,)$$

2. Calculate wave vector of the incident wave

$$k_{y,\mathrm{inc}} \;=\; k_0 n_{\mathrm{inc}}$$

3. Calculate periodic expansion of the transmitted wave vector

$$k_x\,(m) \;=\; -2\pi m / L_x,\;\; m = -\mathrm{floor}[N_x/2], \dots, -1, 0, 1, \dots, \mathrm{floor}[N_x/2]$$

4. Calculate longitudinal wave vector components for the reflection and transmission

$$k_{y,ref}(m) = \sqrt{(k_0 n_{ref})^2 - k_x^2(m)},$$

$$k_{y,trn}(m) = \sqrt{(k_0 n_{trn})^2 - k_x^2(m)}$$

5. Normalize the steady-state fields to the EM source

$$\hat{\mathbf{E}}_{ref}(x,f) = \frac{\mathbf{E}_{ref}(x,f)}{\mathbf{E}_{src}(f)}, \quad \hat{\mathbf{E}}_{trn}(x,f) = \frac{\mathbf{E}_{trn}(x,f)}{\mathbf{E}_{src}(f)}$$

6. Calculate the complex amplitudes of the spatial harmonics

$$\mathbf{S}_{ref}(m,f) = \mathrm{FFT}\left\{\hat{\mathbf{E}}_{ref}(x,f)\right\}, \quad \mathbf{S}_{trn}(m,f) = \mathrm{FFT}\left\{\hat{\mathbf{E}}_{trn}(x,f)\right\}$$

7. Calculate the diffraction efficiencies of the spatial harmonics

$$\mathrm{DE}_{ref}(m,f) = |\mathbf{S}_{ref}(m,f)|^2 . \mathrm{Re}\left[\frac{k_{y,ref}(m)}{k_{y,inc}}\right]$$

$$\mathrm{DE}_{trn}(m,f) = |\mathbf{S}_{trn}(m,f)|^2 . \mathrm{Re}\left[\frac{k_{y,trn}(m)}{k_{y,inc}} \frac{\mu_{ref}}{\mu_{trn}}\right]$$

8. Calculate energy conservation, transmission, and reflection coefficients

$$R(f) = \sum_m \mathrm{DE}_{ref}(m,f), \quad T(f) = \sum_m \mathrm{DE}_{trn}(m,f),$$

$$C(f) = R(f) + T(f)$$

4.RESULTS

The transmission spectrums are calculated for all of our designs with different values of G parameter (distance between dual metallic layers) in TM mode and plotted versus wavelength. The sizes of metal gratings chosen for three different designs are given in this section. We named these three different designs as design A, design B, and design C, respectively.

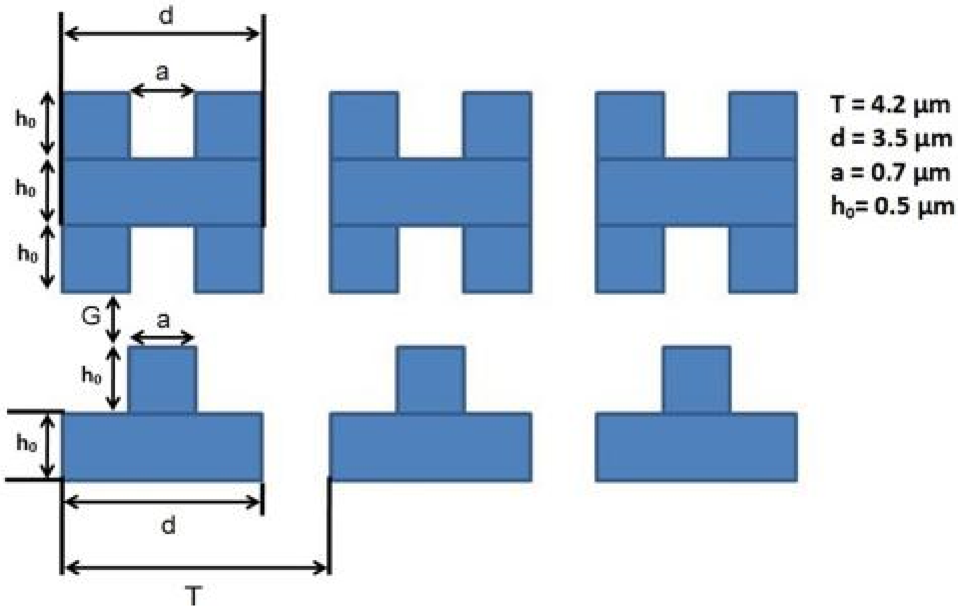

Figure 4.1. Schema of metallic periodic condition for design A.

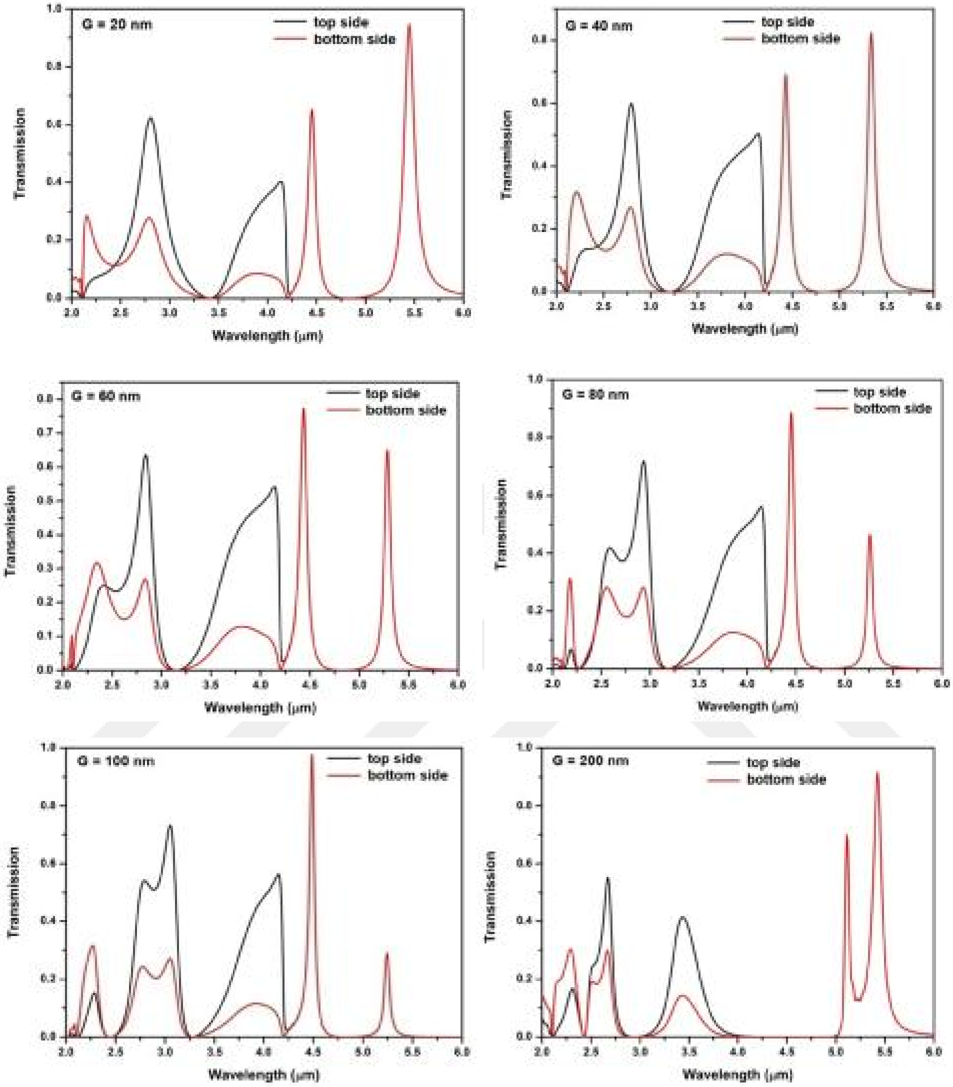

Figure 4.2. FDTD simulation results obtained by MEEP program for the design A.

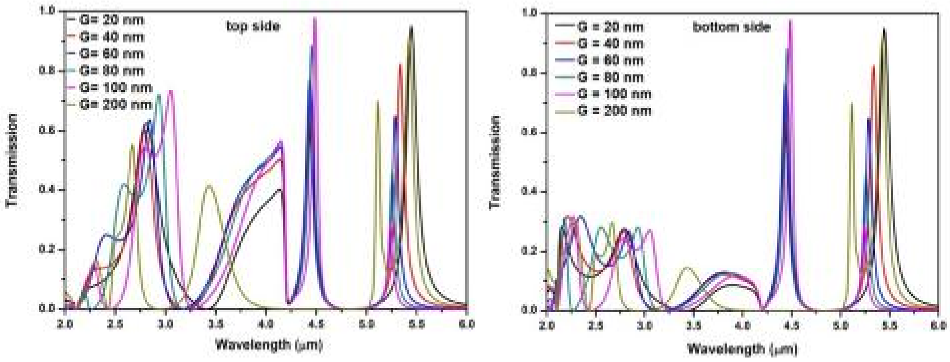

Figure 4.3. All G parameter (distance between dual metallic layers) dependent FDTD simulation results for design A.

The transmission spectrum of design A is calculated for different values of G parameter in TM mode and plotted versus wavelength as shown in figure 4.3. It can be said that there is only one asymmetric transmission feature with the maximum transmittances are as large as 0.5 and 0.1 for top side and bottom side respectively in calculated region of wavelength range from 3.25 to 4.25 µm. Further, it may be seen from figure 4.3, that the design A exhibits many narrow photonic band gaps can be seen in simulation results.

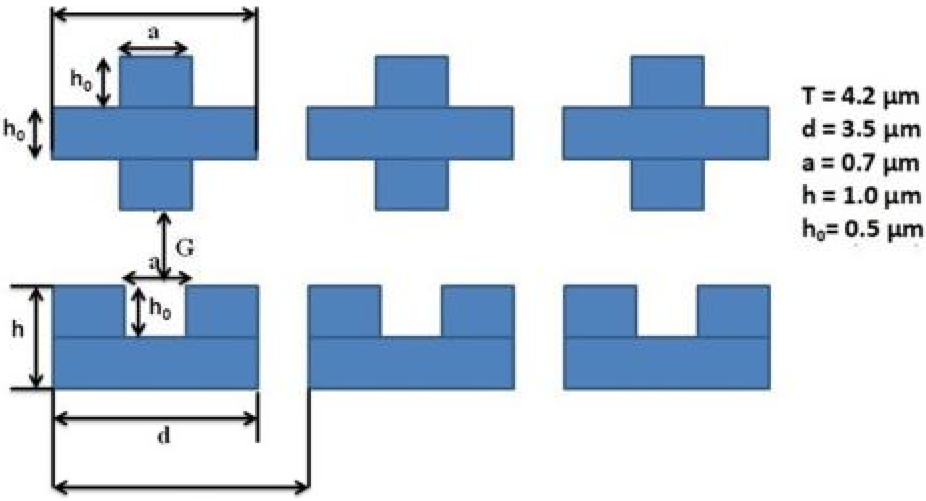

Figure 4.4. Schema of metallic periodic condition for design B.

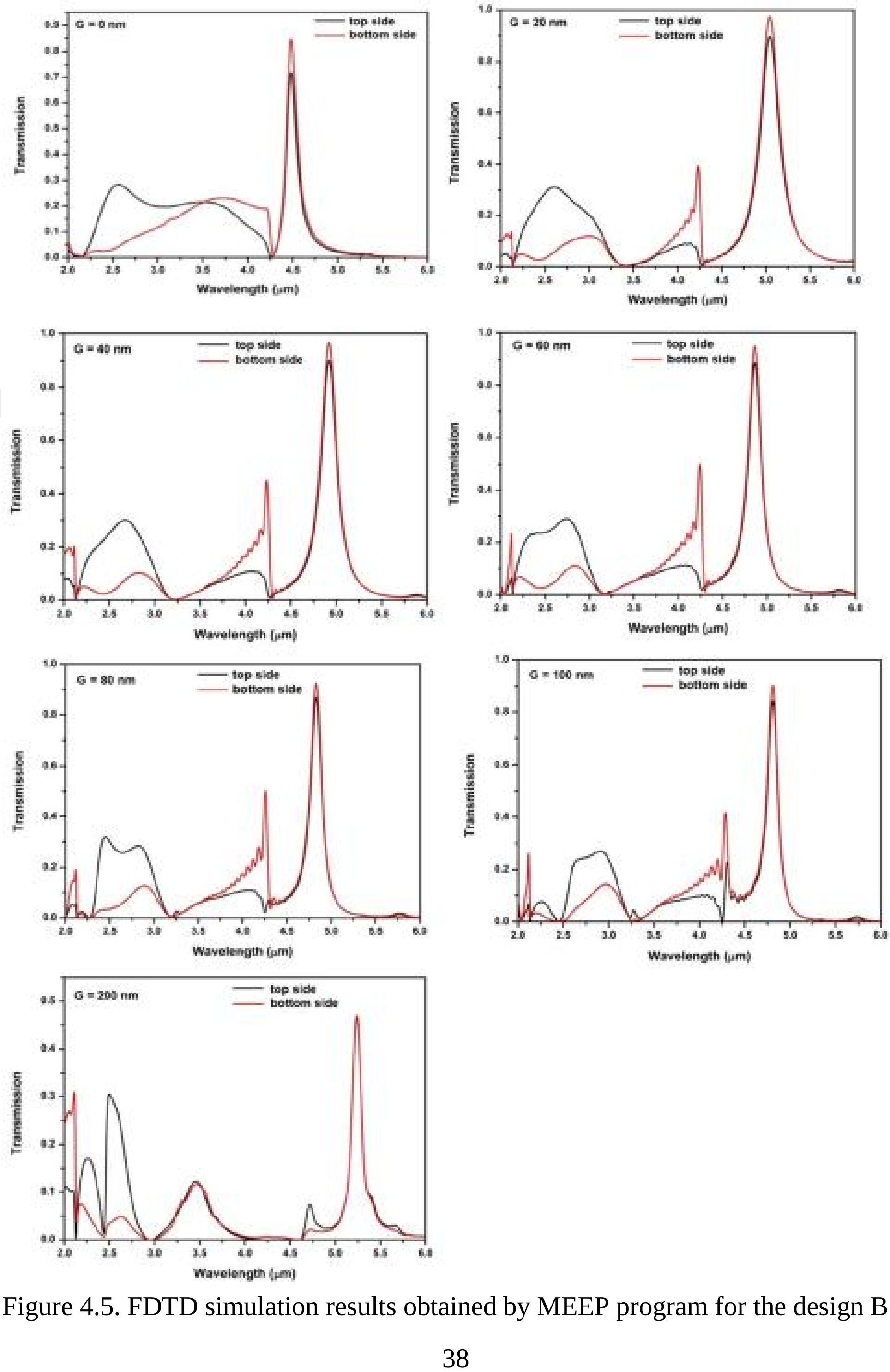

Figure 4.5. FDTD simulation results obtained by MEEP program for the design B.

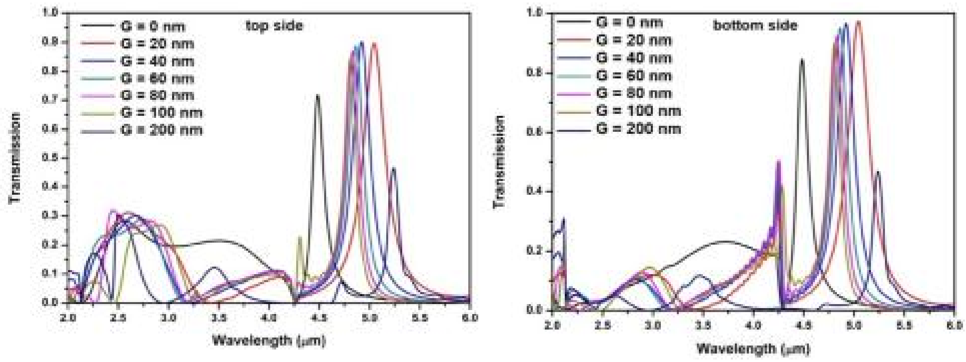

Figure 4.6. All G parameter (distance between dual metallic layers) dependent FDTD simulation results for design B.

The transmission spectrum of design B is calculated for different values of G parameter in TM mode and plotted versus wavelength for top side and bottom side from left to right respectively as shown in figure 4.6. According to this graph, there is no certain evidence of asymmetric transmission with several band gaps and a maximum of filtering feature around wavelength of 5 μm.

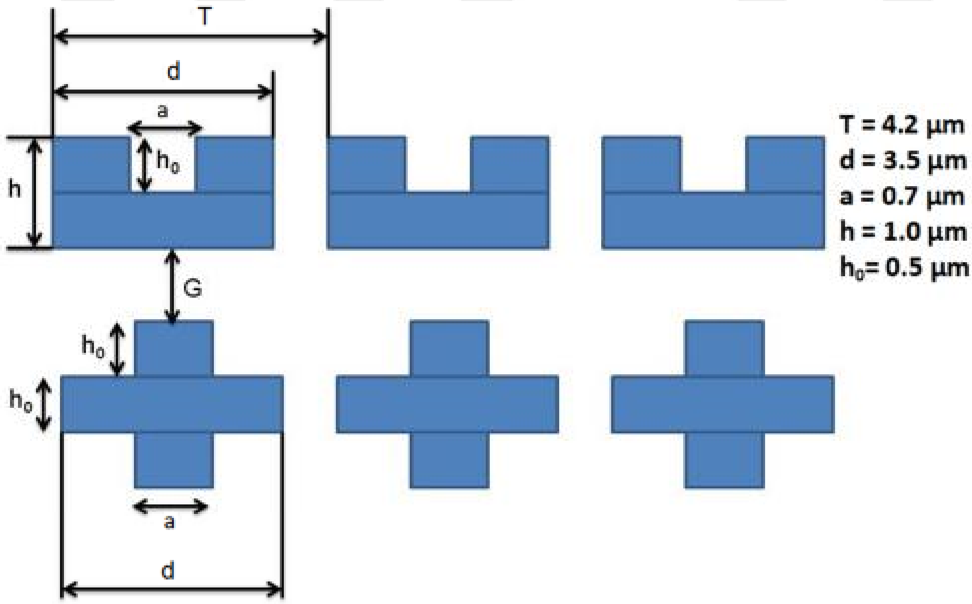

Figure 4.7. Schema of metallic periodic condition for design C.

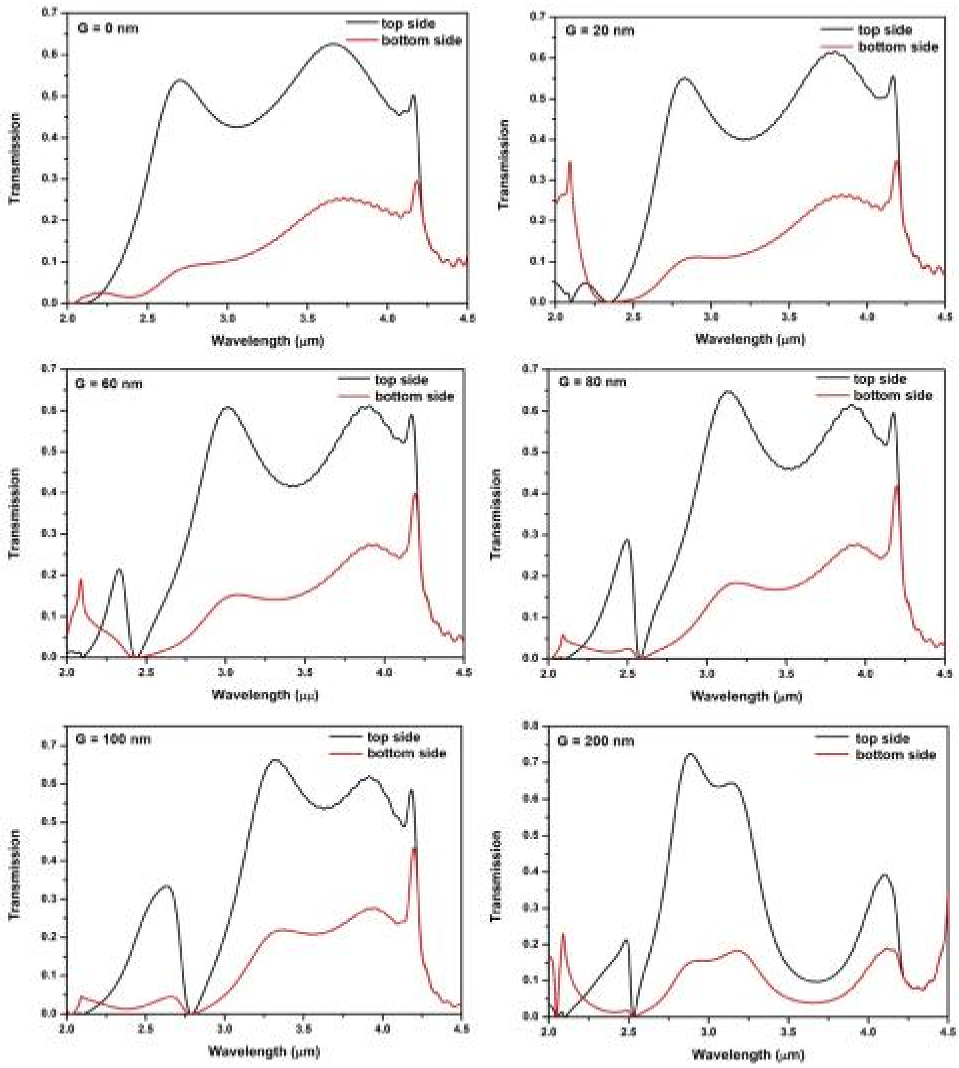

Figure 4.8. FDTD simulation results obtained by MEEP program for the design C.

The transmission spectrum of design C is calculated for different values of G parameter in TM mode and plotted versus wavelength as shown in figure 4.8. It can be clearly seen that an asymmetric transmission behavior can be obtained for a large range of wavelength for all G parameters. When the graphs of the simulation results are compared, it can be said that the most efficient asymmetric characteristic is founded for G=200 nm as 0.75 and 0.15 for top side and bottom side respectively.

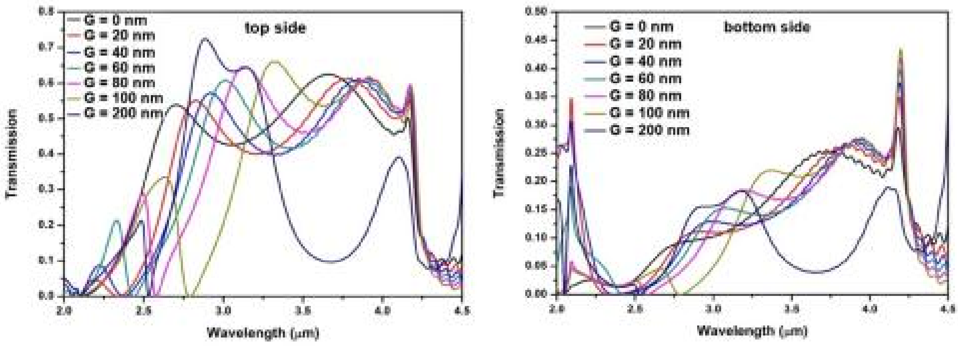

Figure 4.9. All G parameter (distance between dual metallic layers) dependent FDTD simulation results for design C.

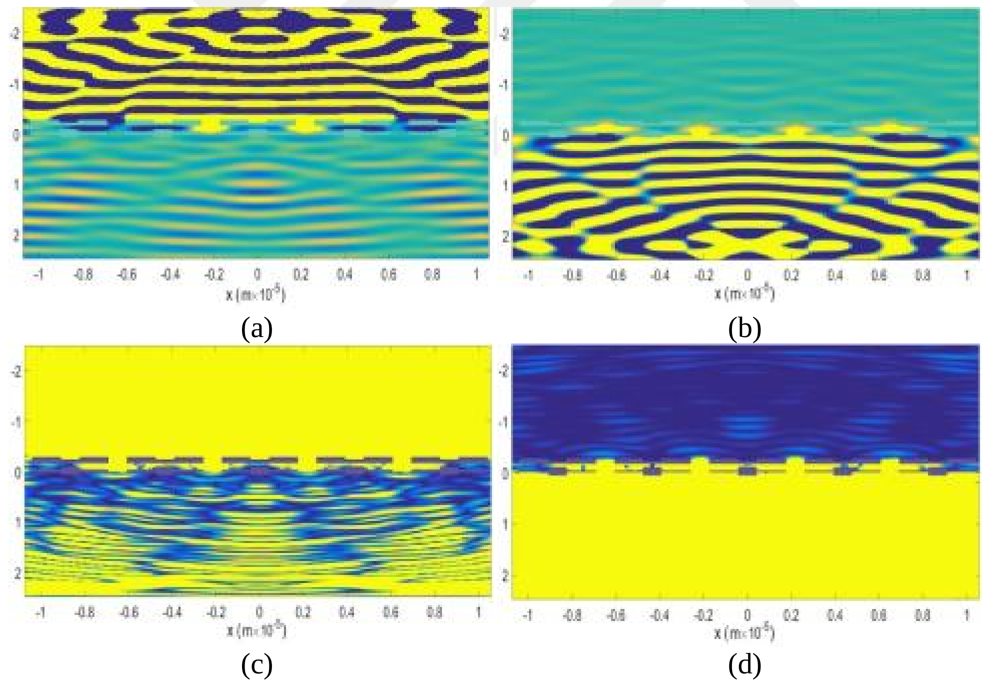

Figure 4.10. Ez field (TM) mode propagation (a) incidence from top side, (b) incidence from bottom side. Poynting vector distribution (c) incidence from top side, (d) incidence from bottom side for design C (G=200nm, λ= 2.9 μm).

The wave propagations and Poynting vector distributions from top side and bottom side are obtained by MATLAB and shown in figure 4.10. According to these simulation results, the intensities of field distribution and Poynting vector in the transmission region confirm the transmittance result is calculated for design C with G=200nm, λ= 2.9 µm by using the MEEP program.

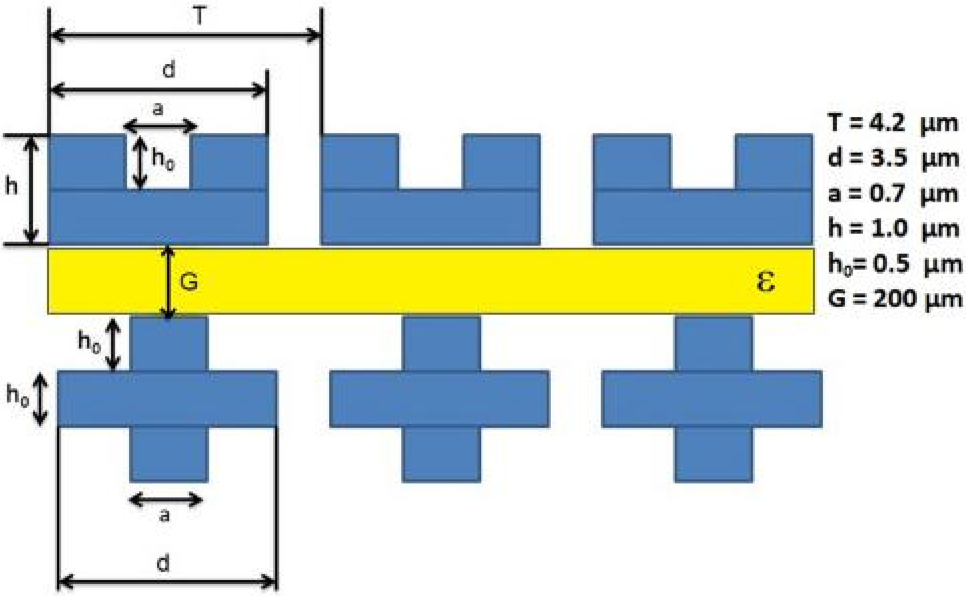

Figure 4.11. Schema of metallic periodic condition for design C with intermediate dielectric material.

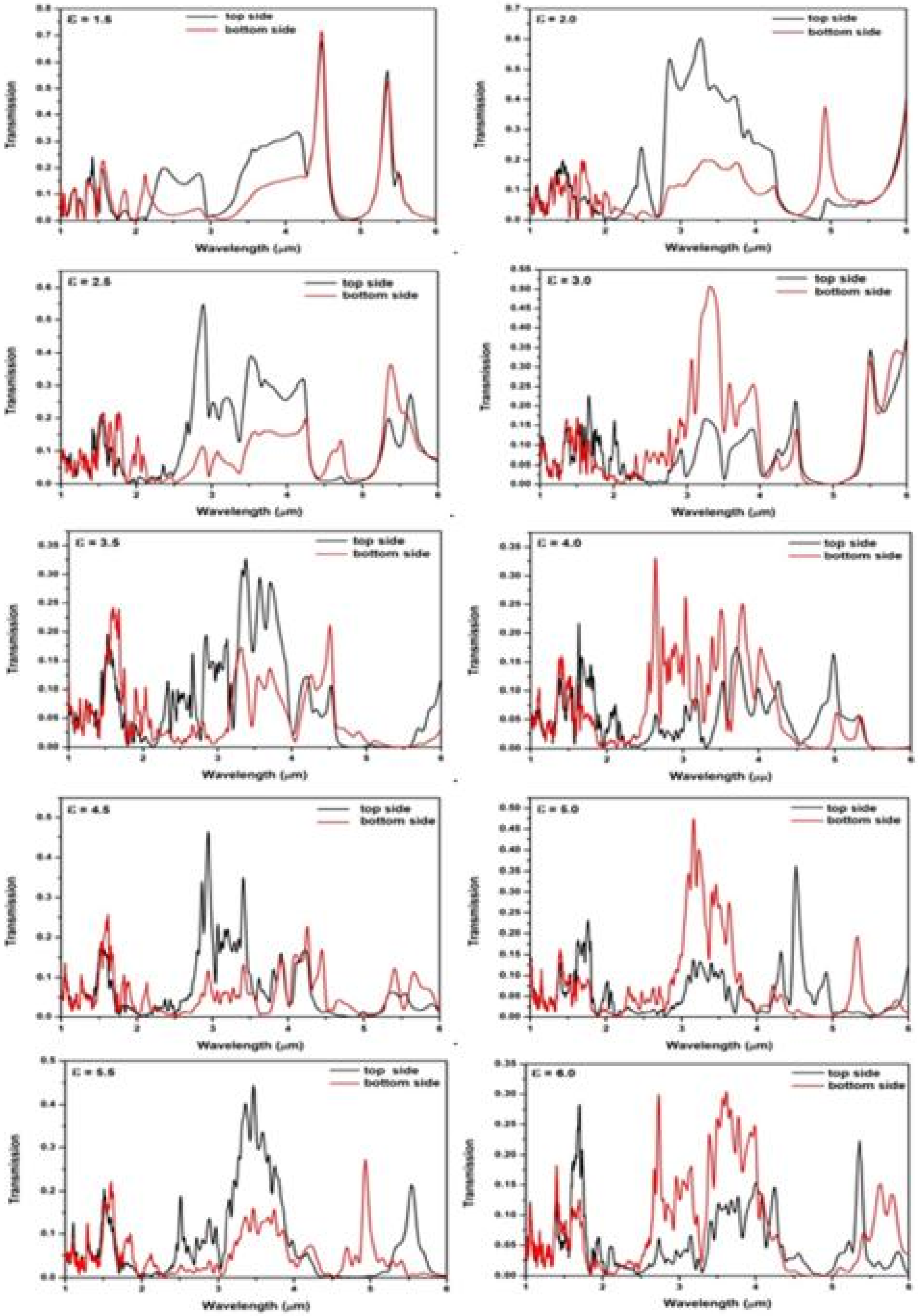

Figure 4.12. FDTD simulation results obtained by MEEP program for the design C with intermediate dielectric material.

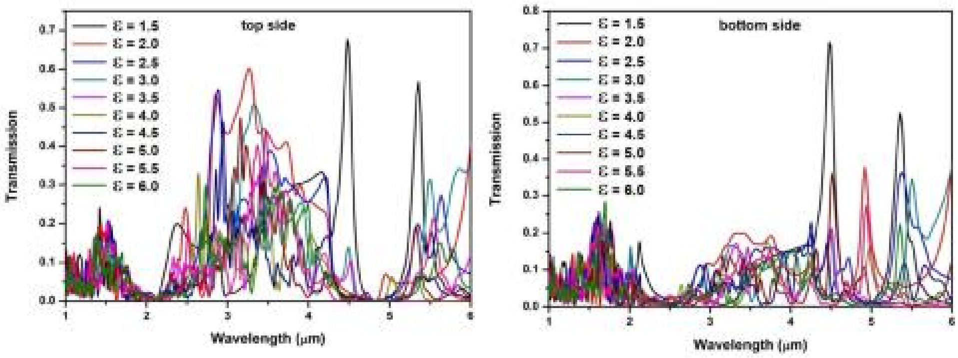

Figure 4.13. All ε parameter dependent FDTD simulation results for design C with intermediate dielectric material.

The effects of an intermediate dielectric material between dual metallic layer have been investigated for design C with G=200 nm. The all simulation results are calculated for different dielectric constants of the intermediate material in TM mode and plotted versus wavelength as shown in figure 4.13. According to simulation results, the intermediate material has demolished the behavior of asymmetric transmission in dual metallic layer of design C for all values of dielectric constant. Also, it is not possible to talking about a useful feature because there is no definite asymmetric transmission, band gap, and maximum for filtering.

5. CONCLUSION

The aim of this thesis was to obtain an asymmetric transmission behavior in the 2-D dual metallic photonic crystals. For this purpose, we designed three novel dual metallic structures and analyzed the numerical results of electromagnetic wave propagation for TM mode. Firstly, the distance between dual metallic layers was modified to obtain the asymmetric transmission. It is possible to say that we could not obtain an effective asymmetric transmission behavior for our design A and B. Nevertheless, we have carried out an asymmetric transmission behavior in design C for a large range of wavelength for all G values. We have also checked the most effective parameters of design C (G=200nm, λ= 2.9 µm) by MATLAB simulations. The MATLAB results are consistent with the MEEP results. As a further work, we have studied on the effects of an intermediate dielectric material between dual metallic layer of design C for G=200 nm. But the transmission spectrum results show that the intermediate material has almost demolished the behavior of asymmetric transmission in the structure of design C.

The asymmetric transmission means that an electromagnetic propagation is completely transmitted in one direction, but blocked in other direction. This feature may be utilized to design the optical diodes (Scalora, 1994) for light based integrated circuits. Consequently, the transmission spectrum of design C may reveal the optical diode like transmission behavior around 3 µm. There can be found many studies on such optical diodes in literature (Biancalana, 2008: Wang, 2011: Kurt, 2012: Stolarek, 2013). Although our goal was to achieve an asymmetric transmission behavior, the design A and B have shown a sharp filtering feature (Wang, 1995: Hu, 2015) from top side and bottom side for around 5.5 and 5 µm, respectively.

REFERENCES

Abdel Malek, F., 2011. Design of a Novel Left-Handed Photonic Crystal Sensor Operating in Aqueous Environment. IEEE Photonics Technology Letters, 23(3), 188-190.

Allen, T., 2005. Computational Electrodynamics: The Finite-Difference Time-Domain Method Third Edition. Artech House.

Ampere, A. M., 1820. Memoire presente a 'Academie royale des sciences, Annales de Chimie tome XV.

Baohua, J., Buso, D., Jiafang, L., Min, G., 2009. Active Three Dimensional Photonic Crystals with High Third Order Nonlinearity in Telecommunication. Proceedings of the IEEE International Conference on Lasers and Electro Optics, 1-2.

Benisty, H., Cambournac, C., Laere, F. V., Thourhout, D. V., 2010. Photonic Crystal Demultiplexer with Improved Crosstalk by Second-Order Cavity Filtering. Journal of Light Wave Technology, 28(8), 1201-1208.

Berenger, J. P., 1994. A Perfectly Matched Layer for the Absorption of Electromagnetic Waves. J. Comput. Phys. Vol., 114 pp. 185–200.

Biancalana F., 2008. All-optical diode action with quasiperiodic photonic crystals. J. Appl. Phys., 104(9), 093113.

Borel, P. I., Frandsen, L. H., Harpoth, A., Kristensen, M., Jensen, J. S., Sigmund O., 2005. Topology Optimized Broadband Photonic Crystal Y-Splitter. Electronics Letters, 41(2), 69-71.

Bruyant, A., Lerondel, G., Reece, P. J., Gal, M., 2003. All-Silicon Omnidirectional Mirrors Based on One-Dimensional Photonic Crystals. Applied Physics Letters, 82(19), 3227-3229.

Chen, M. C., Luan, P. G., Lee, C. T., 2003. Novel Design of Organic One-Dimensional Photonic Crystal Filter. Proceedings of the 5th IEEE International Conference on Lasers and Electro-Optics, 2, 1-4.

Cheng, C., Chen, J., Shi, D. J., Wu, Q. Y., Ren, F. F., Xu, J., Fan, Y. X., Ding, J., Wang, H. T., 2008. Physical Mechanism of Extraordinary Electromagnetic Transmission in Dual-Metallic Grating Structures. Phys. Rev. B 78, 075406.

Cheng, C., Chen, J., Wu, Q. Y., Ren, F. F., Xu, J., Fan, Y. X., Wang, H. T., 2007. Controllable Electromagnetic Transmission Based on Dual-Metallic Grating Structures Composed of Subwavelength Slits. Appl. Phys. Lett. 91, 111111.

Coulomb, C.A., 1785. Memior.

Deubel, M., Von Freymann, G., Wegener, M., Pereira, S., Busch, K., Soukoulis, C. M., 2004. Direct Laser Writing of Three Dimensional Photonic Crystal Templates for Photonic Bandgaps at Telecommunication Wavelengths. Proceedings of the IEEE International Conference on Lasers and Electro Optics, 1-3.

Djavid, M., Ghaffari, A., Monifi, F., Abrishamian, M. S., 2008. Photonic Crystal Power Dividers Using L-Shaped Bend Based on Ring Resonators. Journal of Optical Society of America B, 25(8), 1231-1235.

Faraday, M., 1834. Philosophical Transactions of the Royal Society.

Gannat, G. A., Pinto, D., Obayya, S. S. A., 2009. New Configuration for Optical Waveguide Power Splitters. IET Optoelectronics, 3(2), 105-111.

Gauss, C. F., 1839. Allgemeine Theorie des Erdmagnetismus.

Ge, J.; and Yin, Y., 2011. Responsive Photonic Crystals. Angewandte Chemie International Edition, 50 (7), 1492-1522.

Hu, R., Liang, Y., Qian S., Peng, W., 2015. W. Dual-band Bandpass Filter Based on Compound Metallic Grating Waveguide Structure, Optics Communications, 336, 110–115.

Inoue, K.; and Ohtaka, K., 2004. Two-Dimensional Photonic Crystals. Springer Series in OPTICAL SCIENCES, vol 94.

Joannopoulos, J. D., Johnson, S. G., Winn, J. N., Meade, R, D., 2008. Photonic Crystals Molding the Flow of Light Second Edition. Princeton University Press.

John, S., 1987. Strong Localization of Photons in Certain Disordered Dielectric Superlattices. Physics Review Letters, 58(23), 2486-2489.

Kraus, J. D., 2000. Electromagnetics Fourth Edition. McGraw-Hill, New York.

Krauss, T. F., De La Rue, R. M., Brand, S., 1996. Two-Dimensional Photonic-Bandgap Structures Operating at Near-Infrared Wavelengths. Nature, 383 (6602), 699-702.

Kurt, H., Yilmaz, D., Akosman, A. E., Ozbay, E., 2012. Asymmetric Light Propagation in Chirped Photonic Crystal Waveguides. Optics Express, Vol. 20, No. 18.

Lee, H. Y., Cho, S. J., Nam, G. Y., Lee, W. H., Baba, T., Makino, H., Cho, M. W., Yao, T., 2005. Multiple Wavelength Transmission Filters Based on Si-SiO2 One Dimensional Photonic Crystals. Journal of Applied Physics, 97(10), 103111-103111.

Li, Y., Xiang, Y., Wen, S., Yong, J., Fan, D., 2011. Tunable Terahertz Mirror and Multi Channel Terahertz Filter Based on One Dimensional Photonic Crystals Containing Semiconductors. Journal of Applied Physics, 110(7), 073111-073111.

Liu, J. M., 2005. Photonic Devices. Cambridge University Press, Cambridge.

Liu, R. J., Li, Z. Y., Feng, Z. F., Cheng, B. Y., Zhang, D. Z., 2008. Channel Drop Filters in Three Dimensional Woodpile Photonic Crystals. Journal of Applied Physics, 103(9), 094514-094514.

Lu, T. W., Chiu, L. H., Lin, P. T., Lee, P. T., 2011. One-Dimensional Photonic Crystal Nanobeam Lasers on a Flexible Substrate. Applied Physics Letters, 99(7), 071101-071101.

Ma, Z.; and Ogusu, K., 2011. Channel Drop Filters Using Photonic Crystal Fabry–Perot Resonators. Optics Communications, 284(5), 1192-1196.

Mahmoud, M. Y., Bassou, Z. M., Taalbi, A., Chekroun, Z. M., 2012. Optical Channel Drop Filter Based on Photonic Crystal Ring Resonators. Optics Communications, 285(1), 368-372.

Maxwell, J. C., 1954. Dover Publications, New York.

Moghaddam, M. K., Attari, A. R., Mirsalehi, M. M., 2010. Improved Photonic Crystal Directional Coupler with Short Length. Photonics and Nanostructures-Fundamentals and Applications, 8(1), 47-53.

Moghaddam, M. K., Attari, A. R., Mirsalehi, M. M., 2010. Improved Photonic Crystal Directional Coupler with Short Length. Photonics and Nanostructures-Fundamentals and Applications, 8(1), 47-53.

Moore, G. E., 1975. Progress in Digital Integrated Electronics. Tech. Dig. IEEE Int. Electron Devices Meeting, pp. 11–13.

Nemec, H., Duvillaret, L., Garet, F., Kuzel, P., Xavier, P., Richard, J., Rauly, D., 2004. Thermally Tunable Filter for Terahertz Range Based on a One-Dimensional Photonic Crystal with a Defect. Journal of Applied Physics, 96(8), 4072-4075.

Ogawa, S., Tomoda, K., Noda, S., 2002. Effects of Structural Fluctuations on Three Dimensional Photonic Crystals Operating at Near-Infrared Wavelengths. Journal of Applied Physics, 91(1), 513-515.

Ohkubo, H., Ohtera, Y., Kawakami, S., Chiba, T., 2004. Transmission Wavelength Shift of +36 nm Observed with Ta2O5-SiO2 Multichannel Wavelength Filters Consisting of Three Dimensional Photonic Crystals. IEEE Photonic Technology Letters, 16(5), 1322-1324.

Olyaee, S.; and Dehghani, A. A., 2012. High Resolution and Wide Dynamic Range Pressure Sensor Based on Two-Dimensional Photonic Crystal. Photonic Sensors, 2(1), 92-96.

Pedrotti, F. L.; and Pedrotti, L. S., 2007. Introduction to Optics Third Edition. Prentice Hall, Upper Saddle River, NJ.

Popovic, Z.; and Popovic, B. D., 2000. Introductory Electromagnetics. Prentice-Hall, Upper Saddle River, NJ.

Rawal, S.; and Sinha, R. K., 2009. Design, Analysis and Optimization of Silicon-on-Insulator Photonic Crystal Dual Band Wavelength Demultiplexer. Optics Communications, 282(19), 3889-3894.

Rayleigh, J. W. S., 1888. On The Remarkable Phenomenon of Crystalline Reflexion Described by Prof. Stokes. Philosophical Magazine, 26:256-265.

Robinson, S.; and Nakkeeran, R., 2013. Photonic Crystal Ring Resonator Based Optical Filters (Edited by Vittorio M. N. Passaro). Advances in Photonic Crystals, InTech, ISBN 978-953-51-0954-9.

Scalora, M., Dowling, J. P., Bowden, C. M., Bloemer, M. J., 1994. The Photonic Band Edge Optical Diode. J. Appl. Phys., 76(4), 2023–2026.

Stolarek, M., Yavorskiy, D., Kotyński, R., Zapata Rodríguez, C. J., Łusakowski, J., Szoplik, T., 2013. Asymmetric Transmission of Terahertz Radiation through a Double Grating. Optics Letters, vol. 38, pp 839-841.

Taflove, A.; and Brodwin, M. E. E., 1974. Numerical Solution of Steady-State Electromagnetic Scattering Problems Using the Time-Dependent Maxwell’s Equations. Microw. Theory Tech. IEEE Trans., vol. 23, no. 8, pp. 623–630.

Taflove, A.; and Hagness, S. C., 2000. Computational Electrodynamics: The Finite Difference Time-Domain Method 2nd edn. Boston, MA: Artech House Publishers.

Taniyama, H., 2002. Waveguide Structures Using One-Dimensional Photonic Crystal. Journal of Applied Physics, 91(6), 3511-3515.

Wang, C., Zhou, C. Z., Li, Z. Y., 2011. On-chip Optical Diode Based on Silicon Photonic Crystal Heterojunctions. Opt. Express, 19(27), 26948–26955.

Wang, Q., Cui, Y., Zhang, H., Yan, C., Zhang, L., 2010. The Position Independence of Heterostructure Coupled Waveguides in Photonic Crystal Switch. Optik, 121(8), 684-688.

Wang, S. S., Magnusson, R., 1995. Multilayer Waveguide-grating Filters, Appl.Opt., 34, 2414.

Wartak, M. S., 2013. Computational Photonics: An Introduction with MATLAB. Cambridge University Press.

Xu, J., Cheng, C., Kang, M., Chen, J., Zheng, Z., Fan, Y. X., Wang, H. T., 2011. Unidirectional Optical Transmission in Dual-Metal Gratings in the Absence of Anisotropic and Nonlinear Materials. Opt. Lett. 36, 1905.

Yablonovitch, E., 1987. Inhibited Spontaneous Emission in Solid-State Physics. Physics Review Letters, 58(20), 2059-2062.

Yablonovitch, E., Gmitter, T. J., Leung, K. M., 1991. Photonic Band Structure: The Face-Centered-Cubic Case Employing Nonspherical Atoms. Physical Review Letters, 67 (17), 2295.

Yang, Y. L., Hou, F. J., Wu, S. C., Huang, W. H., Lai, M. C., Huang, Y. T., 2009. Fabrication and Characterization of Three Dimensional All Metallic Photonic Crystals for Near Infrared Applications. Applied Physics Letters, 94(4), 041122-041122.

Yee, K. S., 1966. Numerical Solution of Initial Boundary Value Problems Involving Maxwell’s Equations in Isotropic Media. IEEE Transscations Antennas Propag.

BIOGRAPHY

Fulya was born in Ceyhan on September 20th, 1985. She completed elementary and high school in Ceyhan than entered Physics Department of Çukurova University in 2003. She graduated from this program in 2007. After university, she worked as Physics teacher for 5 years. She joined to Electrical Electronic Engineering Department of Hakkari University as research assistant in 2013. She is currently MS student in Electrical Electronics Engineering Department of Çukurova University in Adana, Turkey.